Molecular Phylogenetics and Evolution 197 (2024) 108109

Contents lists available at ScienceDirect

Molecular Phylogenetics and Evolution

journal homepage: www.elsevier.com/locate/ympev

Phylogeny and biogeography of harmochirine jumping spiders (Araneae: Salticidae)

Guilherme H.F. Azevedo [a,*], Marshal Hedin [a], Wayne P. Maddison [b]

[a] Dept of Biology, San Diego State University, San Diego, CA 92182, United States
[b] Departments of Zoology and Botany and Beaty Biodiversity Museum, University of British Columbia, 6270 University Boulevard, Vancouver, British Columbia V6T 1Z4, Canada

ARTICLE INFO

Keywords:
Plexippini
Harmochirina
Molecular phylogeny
Pacific Islands
Molecular clock rate estimation
Ultraconserved elements

ABSTRACT

We use ultraconserved elements (UCE) and Sanger data to study the phylogeny, age, and biogeographical history of harmochirine jumping spiders, a group that includes the species-rich genus *Habronattus*, whose remarkable courtship has made it the focus of studies of behaviour, sexual selection, and diversification. We recovered 1947 UCE loci from 43 harmochirine taxa and 4 outgroups, yielding a core dataset of 193 UCEs with at least 50 % occupancy. Concatenated likelihood and ASTRAL analyses confirmed the separation of harmochirines into two major clades, here designated the infratribes Harmochirita and Pellenita. Most are African or Eurasian with the notable exception of a clade of pellenites containing *Habronattus* and *Pellenattus* of the Americas and *Havaika* and *Hivanua* of the Pacific Islands. Biogeographical analysis using the DEC model favours a dispersal of the clade's ancestor from Eurasia to the Americas, from which *Havaika*'s ancestor dispersed to Hawaii and *Hivanua*'s ancestor to the Marquesas Islands. Divergence time analysis on 32 loci with 85 % occupancy, calibrated by fossils and island age, dates the dispersal to the Americas at approximately 4 to 6 million years ago. The explosive radiation of *Habronattus* perhaps began only about 4 mya. The phylogeny clarifies both the evolution of sexual traits (e.g., the terminal apophyses was enlarged in *Pellenes* and not subsequently lost) and the taxonomy. *Habronattus* is confirmed as monophyletic. *Pellenattus* is raised to the status of genus, and 13 species moved into it as new combinations. *Bianor stepposus* Logunov, 1991 is transferred to *Sibianor*, and *Pellenes bulawayoensis* Wesołowska, 1999 is transferred to *Neaetha*. A molecular clock rate estimate for spider UCEs is presented and its utility to inform prior distributions is discussed.

1. Introduction

The large family of jumping spiders (Salticidae; >6000 species described) shows a strong biogeographical pattern, with major clades largely restricted to specific continental regions (Maddison and Hedin, 2003b; Bodner and Maddison, 2012; Maddison, 2015). This pattern is broken by a few lineages occurring far from their close relatives, e.g., *Habronattus*, F.O. Pickard-Cambridge, 1901 in the Americas, far from Africa and Eurasia where most other Plexippini occur; *Attulus* Simon, 1889 in Eurasia, far from the Americas where other Amycoida occur; and *Myrmarachne* MacLeay, 1839, in Asia and beyond, far from Australasia where most other Astioida occur. Each of these isolated genera has been interpreted as having dispersed away from its relatives (Maddison, 2015), but no formal biogeographic analyses have been done. The first mentioned, *Habronattus* (the "paradise spiders"), is a group of about 100 species studied intensively for their elaborate male ornamentation and courtship behaviour (e.g., Peckham and Peckham, 1889, 1890; Elias et al., 2003, 2012; Hebets and Maddison, 2005; Taylor and McGraw, 2013), sensory physiology (Zurek et al., 2015; Taylor et al., 2016), chromosomes (Maddison and Leduc-Robert, 2013), and patterns of diversification (Maddison and McMahon, 2000; Masta and Maddison, 2002; Leduc-Robert and Maddison, 2018; Hedin et al., 2020; Bougie et al., 2021; Bougie et al, 2024). Partly because of the breadth of biological studies focused on it, *Habronattus* has received more phylogenetic attention than for any other genus of salticids, with both morphological and genomic analyses (Griswold, 1987; Maddison and Hedin, 2003a; Leduc-Robert and Maddison, 2018). However, our phylogenetic knowledge of the broader group in which it lies, the Harmochirina, has been limited by sampling biased to the Americas.

One of our primary goals here is to study the phylogenetic context of

* Corresponding author.
E-mail address: ghfazevedo@gmail.com (G.H.F. Azevedo).

https://doi.org/10.1016/j.ympev.2024.108109
Received 17 February 2024; Received in revised form 2 May 2024; Accepted 17 May 2024
Available online 18 May 2024

Habronattus, to better understand when, where, and from what ancestral conditions this remarkable group arose. The genus has long been considered related to *Pellenes* Simon, 1876 (Peckham and Peckham, 1909; Lowrie and Gertsch, 1955; Griswold, 1987), a diverse group of mostly Old-World species now divided into multiple subgenera (Logunov et al., 1999; Prószyński, 2016; Maddison, 2017). Together with the Afro-Eurasian *Neaetha* Simon, 1884, *Pellenes* and *Habronattus* are part of a harmochirine subgroup that Maddison (2015) called the "pellenines". The recent molecular phylogenetic sampling of non-*Habronattus* pellenines, however, has missed much of its diversity, including only a few species of *Pellenes* and *Havaika* (Maddison and Hedin, 2003b; Arnedo and Gillespie, 2006; Maddison et al., 2008), only one of which is represented by more than a few genes (Leduc-Robert and Maddison, 2018).

In this paper, we use sequence capture of ultraconserved elements (UCEs) and Sanger sequencing data to elucidate the phylogenetic relationships and biogeographic history of harmochirine jumping spiders. More specifically, we aim to test if the subgroups harmochirines s. str. and pellenines (Maddison, 2015) are reciprocally monophyletic; test the monophyly of *Pellenes* and *Habronattus*; determine the sister group to *Habronattus*; clarify the phylogenetic position of several taxa, including *Modunda* Simon, 1901 and the Pacific Islands taxa (*Havaika* Prószyński, 2002 and *Hivanua* Maddison, 2024); and adjust the taxonomy accordingly. We explore their biogeographical history by estimating a dated phylogeny and using Dispersal-Extinction-Cladogenesis (DEC; Ree and Smith, 2008) models to test routes of colonization among Afro-Eurasia, the Americas, and the Pacific Islands of the Hawaiian and Marquesan archipelagos. In addition, we provide a molecular clock rate estimation for a subset of spider UCE loci as well as for the COI and 28S loci, which can be used in future studies with taxa for which fossils are unavailable. We also discuss the implications of our phylogenetic findings for the evolution of sexual traits (genitalia and ornaments).

2. Material and methods

2.1. Taxon sampling

We generated original UCE sequence-capture data for 47 specimens representing at least 40 species from 10 harmochirine genera (out of 15 genera listed by Maddison, 2015) and 4 outgroups. To this we added UCE data from 2 harmochirine species downloaded from the Sequence Read Archive (SRA). We also used Sanger data, downloaded from Barcode of Life Data (BOLD) and GenBank, of the commonly used 28S, 16S-ND1 and COI loci from at least 11 additional species of harmochirines. Details regarding sampling information, including accession numbers can be found in Supplemental Material File S1. That file also indicates the translation between a taxon's confirmed name as shown in the figures and the preliminary names used in data files and analyses.

2.2. UCE data

We extracted genomic DNA using the Qiagen DNeasy blood and tissue kit (Qiagen, Valencia, CA, USA). UCE libraries were either prepared at the Hedin Lab (San Diego State University, SDSU), Arbor Biosciences (Ann Arbor, MI, USA) or RAPiD Genomics LLC (Gainesville, Fl) following protocols of Starrett et al. (2017) with modifications of Kulkarni et al. (2020). UCEs were captured using the MYbaits (Arbor Biosciences) Spider v.1 kit (Kulkarni et al., 2020). Sequencing was conducted at either the U.C. Davis Genome Center (Davis, CA), RAPiD Genomics or Arbor Biosciences, on Illumina HiSeq platforms. Bioinformatic analyses were done on the Mesxuuyan High Performance Computing cluster at SDSU.

Trimmomatic v0.39 (Bolger et al., 2014) was used to clean fastq reads with configuration "2:30:10:2:keepBothReads LEADING:5 TRAILING:15 SLIDINGWINDOW:4:15 MINLEN:40". SPAdes v3.15.2 (Bankevich, 2012) was used for assembling contigs with flags "–sc –-careful –-cov-cutoff auto". Assembled contigs were processed using the Phyluce v1.7.1 pipeline (Faircloth, 2016). We used the blended UCEs probe file from Maddison et al. (2020) for matching contigs to probes using min-coverage 80 and min-identity 80. UCE loci present in fewer than four taxa were discarded. Alignments were performed with MAFFT v7.475 (Katoh and Standley, 2013) as implemented in Phyluce. Alignments were trimmed with Gblocks v.0.91b (Castresana, 2000) with options "–b1 0.5 –-b2 0.55 –-b3 10 –-b4 4", and CIAlign v1.0.18 (Tumescheit et al., 2022) with flags "–remove_divergent –-remove_divergent_minperc 0.75 –-remove_insertions –-insertion_min_perc 0.25 –-crop_ends –-remove_short –-remove_min_length '10 % of alignment length' –-crop_divergent". Suspected paralogues were removed in two steps. First, we estimated gene trees for each UCE locus using IQ-TREE v2.1.2 (Nguyen et al., 2015) with flags "-m GTR + F + G" and used TreeShrink (Mai and Mirarab, 2018) with option "-q 0.15" to remove a taxon's sequence in a gene if it was on a long branch. Second, some entire loci were discarded if their gene tree showed any remaining branches that were longer than 50 % of the total gene tree length. The second step was necessary after we inspected alignments and gene trees and noticed some very long internal branches (>50 % of tree length) not removed by TreeShrink, perhaps because of persistent paralogy. This was performed with a custom python program (available at https://doi.org/10.5061/dryad.7wm37pw11) that uses the DendroPy (Sukumaran and Holder, 2010) library. A total of 136 alignments were discarded at this second step. The resultant genomic dataset (named UCEsMin4Tax) consisted of 1947 UCE alignments. This dataset was further filtered to include only alignments with a minimum occupancy of 33 % (dataset UCEs33p), 50 % (dataset UCEs50p) and 85 % (dataset UCEs85p).

2.3. Mitochondrial genes and commonly used markers from UCE libraries

To retrieve approximately complete mitogenomes from UCE libraries as "bycatch", we first downloaded published complete mitochondrial sequences available on GenBank for *Carrhotus xanthogramma* (accession KP402247), *Epeus alboguttatus* (MH922026) and *Habronattus oregonensis* (AY571145). We also used MitoFinder v1.4 (Allio et al., 2020) with default settings to generate mitochondrial contigs from RNAseq reads of *Pellenattus canadensis* (SRR6381075) using *Habronattus oregonensis* as a reference. We aligned mitochondrial genes plus 12S and 16S rRNA of these four species using MAFFT with the E-INS-I algorithm. Based on these alignments we produced a consensus sequence with CIAlign, which was then used as reference to map clean UCE reads using BWA v0.7.17 (Li, 2013) with option "-B 2". Then we used SAMtools v1.15.1 (Li et al., 2009) to generate a consensus fasta file from the mapped reads. Resultant sequences were aligned with MAFFT using the E-INS-I algorithm and passed through CIAlign for cleaning with the same settings as above. This data matrix, named MitoLoci, included 45 taxa for 15 mitochondrial loci.

We also obtained 28S, 16SND1 and COI bycatch from UCE libraries in the same way as above, but mapped reads against a consensus constructed based on the alignment of all Sanger sequencing data acquired from GenBank for those same gene regions. To clarify the taxonomic placement of some species, these traditional markers obtained as bycatch were added to published Sanger-sequenced data for several harmochirines that were unavailable to us for UCE sequencing, most notably several species of *Sibianor*. This dataset included 63 terminals (dataset 28S_16SND1_COI).

2.4. Gene trees based phylogeny

For estimating a species phylogeny that allows for discordance among gene trees, we first inferred gene trees using individual alignments in the UCEsMin4Tax dataset as input to IQ-TREE v2.1.2 with options "-m MFP –mset mrbayes –-mrate I,G,I + G –B 1000". Resultant gene trees were input into ASTRAL v5.7.3 (Zhang et al., 2018). We measured clade support with the local posterior probability and levels of topological discordance were inferred based on alternative normalized

quartet scores.

We acknowledge that further curation of UCE loci, for example understanding possible linkage, could improve phylogenetic accuracy (Hedin et al., 2019; Van Dam et al., 2021). However, at the time these analyses were conducted there was no good complete annotated genome assembled for Salticidae. Salticids, especially *Habronattus*, have very large genomes (Gregory and Shorthouse, 2003), likely with many duplications and repeat elements. Using distantly-related available genomes could either wrongly merge different copies of duplicated genes, or not merge genes due to lack of matches to the reference genome. Also, previous analyses with Dionycha spiders (Azevedo et al., 2022) only merged on average 62 pairs of UCEs. Therefore, we decided not to use curated UCEs until a better annotated genome for Salticidae and *Habronattus* is available.

2.5. Concatenated phylogenies

For all analyses of concatenated UCE data, we used IQ-TREE v2.1.2 with options "-m MFP −-mrate I,G,I + G −mset mrbayes −B 1000 −-alrt 1000". This parameter setting uses ModelFinder (Kalyaanamoorthy et al., 2017) to search for the best model for each partition (individual UCE or other gene alignments), searches for the maximum likelihood tree, and calculates ultrafast bootstrap approximation (UFBoot) (Minh et al., 2013) and approximate likelihood ratio tests (Guindon et al., 2010) as branch support metrics. For the primary dataset (UCEs50p) we also used IQ-TREE to perform a standard non-parametric bootstrap analysis under the same settings. To explore the sensitivity of phylogenetic results to different datasets, analyses were run for each of the following matrices: UCEs33p, UCEs50p, UCES85p, and MitoLoci.

Analysis of the concatenated legacy loci dataset (28S_16SND1_COI) was done both with IQ-TREE as for the UCE data, and with a RAxML v8.2.12 (Stamatakis, 2014) search constrained to have the bycatch taxa match their 50p UCE topology (a skeletal constraint), leaving the Sanger-sequenced taxa free to move. The RAxML search was partitioned by alignment and used the GTRGAMMAI model.

2.6. Divergence dating and clock rate estimation

We used StarBeast3 (Douglas et al., 2022) to estimate divergence times and molecular clock rates accounting for incomplete lineage sorting. We used the UCE 85 % minimum occupancy matrix combined with COI (from MitoLoci bycatch dataset) and 28S alignments obtained as bycatch (named UCEs85p_COI_28S, 32 loci) for 48 species (*Havaika* sp. [Kauai, d300] had only 3 UCEs and was removed). For all genes we used an GTR + G4 + I model with empirical base frequencies, exponential prior with mean 1 for the instantaneous rate matrix parameters and for the shape of the gamma distributed variation of site rates, and a uniform distribution between 0 and 1 for the proportion of invariant sites. We chose this model because we wanted to account for uncertainty in the substitution model while estimating dates and clock rates. We assumed a strict species tree clock, not only to reduce parameter space but also because we have few calibration points and vague prior information on rate variation and loci rates, which could result in low identifiability of rates and node dates (Rannala, 2002; Dos Reis et al., 2016).

Furthermore, we ran additional analyses with a relaxed clock which could not achieve good convergence, and clock rate parameters showed a bimodal distribution, indicating that there could be two areas of parameter space with the same likelihood. In addition, results seemed to be strongly dependent on the prior distribution of species tree clock rate (input and results available at https://doi.org/10.5061/dryad.7wm37pw11). As suggested by simulations studies, rates and ages estimated with a multispecies coalescent strict clock are accurate even when the true clock is not strict, and a strict clock model is sufficient when substitution rate variation is not the main purpose of the study (Ogilvie et al., 2017).

For each locus we used an exponential prior with mean 0.01 for the gene clock rates, since spider UCEs are mostly conserved, nuclear coding (exonic) regions (Hedin et al., 2019; Zhang et al., 2023). This prior distribution puts a higher probability density on values smaller than 0.03 substitutions per million years. Priors for the species tree model parameters were uniform (0, 1000) for the Yule model speciation rate and Inverse Gamma (alpha = 2, beta = 2) for the population sizes mean. To verify that UCEs used for dating were from coding regions, we performed a BlastX search using default parameters in Geneious Prime (Biomatters Ltd.).

The prior on the root age followed Bodner and Maddison (2012) and Zhang and Maddison (2013) with a minimum of 15 and a maximum of 53 my. The justification for the root minimum is based on the abundance of fossil Salticinae in Dominican amber, including species belonging to the tribe Euophryini (Zhang and Maddison, 2013) which is sister to the Salticini + Plexippini sampled in this study. The maximum of 53 my is based on the absence of Salticinae in the Eocene amber fauna (see discussion about the fossil record in Bodner and Maddison (2012) and Zhang and Maddison (2013)), considering the age of the lowermost Eocene amber deposit in Le Quesnoy, France (Nel et al., 2004). Also, previous molecular dating studies with broader taxa and different methods show that is very unlikely that Salticidae is older than 66 my (Bodner and Maddison, 2012; Zhang and Maddison, 2013; Magalhães et al., 2020). Therefore, the maximum of 53 my is reasonable for the subfamily sample here. *Salticus scenicus* was constrained to be sister to remaining taxa.

Biogeographic node calibration might be challenging, but when critically analyzed and well justified, such as in the case of islands, can provide important information when fossils are unavailable (Heads, 2011; Ho et al., 2015; Landis, 2021). Since the genera *Havaika* and *Hivanua* are each monophyletic (see phylogenetic results below and Arnedo and Gillespie (2006)), it is reasonable and parsimonious to assume that each genus diversified within each respective archipelago and therefore, the age of the oldest emergent island would serve as a maximum age for the first divergence within each genus (Landis, 2021). We used a maximum age of 5.3 My for the most recent common ancestor (MRCA) of sampled *Havaika* and 5.56 My for the MRCA of *Hivanua*, based on the oldest age estimated (mean plus the error from supplemental material in Table 1 in Clouard and Bonneville, 2005) for Kauai and the Marquesan Island Eiao, respectively. Although a process-based biogeographic dating approach (Landis, 2017; Landis, 2021) without making the above assumptions would be very appealing, it would be computationally intense and difficult to perform such an analysis in a coalescent based inference with 32 loci and 48 taxa. To explore the influence of island ages (and to acknowledge that older (now submergent) islands existed in the past) we ran an extra analysis with no island calibration. We also ran an analysis under the prior to check if the data was driving the posterior.

Two independent MCMC runs were performed with 120 million iterations each (after a 60 million generations burn in), with a sampling interval of 1000. Log Combiner 2.6.7 (Drummond and Rambaut, 2007) was used to combine log and tree files, resampling with a frequency of 100000. Tracer 1.7.1 (Rambaut et al., 2018) was used for standard convergence checking and a maximum clade credibility tree was summarized with Tree Annotator 2.6.2 (Drummond and Rambaut, 2007). Input xml files are available at https://doi.org/10.5061/dryad.7wm37pw11.

2.7. Biogeographic analyses

We performed biogeographical analyses in a Bayesian framework with RevBayes v1.0.10 (Hohna et al., 2016) using the DEC model (Ree and Smith, 2008) and based on the Bayesian phylogenetic results from the dating analysis. Similar to the molecular model in the dating analyses (above), we did not test other biogeographical models (such as DIVA-like and BayArea-like), because DEC includes all other models

(Ree and Smith, 2008; Matzke, 2013) and, in a Bayesian analysis, can account for parameter uncertainty when testing each biogeographic hypothesis. The J parameter (jump dispersal; Matzke, 2013) was not included for reasons discussed in Ree and Sanmartín (2018) and commented on in Azevedo et al. (2021) (but see Matzke, 2022). Models with the jump dispersal parameter may underestimate anagenetic range dispersal (which is important to test our hypothesis here) and be statistically degenerate, and the probability of a jump dispersal (i.e., a dispersal quickly followed by a vicariance) is already modeled in the regular DEC model. In any case, we also implemented a reversible jump MCMC in RevBayes to attempt both DEC and DEC + J models and calculate the probability of each model given the data (code and results available at https://doi.org/10.5061/dryad.7wm37pw11).

Using constrained dispersal matrices, we compared six hypotheses of dispersal, diagrammed in the inset of Fig. 5: (H1) the American taxa arrived from Eurasia and the genera in the Pacific arrived there through two independent colonizations, one each for Hawaii and the Marquesas; (H2) the American taxa arrived from Eurasia, the Hawaiian genus (*Havaika*) arrived from America and dispersed to the Marquesas; (H3) same as H2, but with an additional dispersal from Marquesas to America; (H4) the Hawaiian taxa arrived from Eurasia, the Marquesan genus arrived from Hawaii and the American taxa were colonized from Eurasia and from Hawaii; (H5) the same as H4, but with the American continent being colonized from Eurasia and Marquesas; (H6) the same as H5, but with three independent colonizations of the Americas, from Eurasia, from Hawaii and from the Marquesas. Lastly, we also estimated an unconstrained model in which dispersal between all areas are allowed (H0).

For all hypotheses we used a time-heterogeneous dispersal matrix (Landis, 2017; Landis et al., 2018) which only allowed dispersal to the archipelago after the islands were formed – i.e., between 4.9 and 5.3 my for Hawaii and between 5.36 and 5.56 my for Marquesas (minimum and maximum estimates from supplemental material in Table 1 from Clouard and Bonneville, 2005). We also used distance-dependent relative dispersal rates (Landis et al., 2013) determined by the EXP($-\beta$ *distance), where β is a distance scale with a uniform prior distribution between 0 and 20, and distance is the approximate shortest distance between two areas. An exponential prior with mean 1 was used for the extirpation rates and the global biogeographic rate scale parameter. We used an uninformative Dirichlet prior for the root state and for the cladogenetic events. Null range was excluded from the rate matrix since it can cause inaccurate estimations of rates and ranges (Massana et al., 2015). Five areas were used: Africa, Eurasian, Americas, Hawaii and Marquesas. To reduce parameter space, ranges that span more than two areas were not allowed. This seems reasonable since no species is found in more than two areas today. We acknowledge that some North American *Habronattus* species also occur in Hawaii (Prószyński, 2002) and we did not consider this in our analyses. This colonization happened much more recently and it is still to be determined if it was natural or a human induced introduction (Prószyński, 2002; Prószyński, 2008; Hedin et al., 2020). Given that our focus is on relatively ancient, natural dispersal, including this recent colonization could introduce bias and add unnecessary complexity to analyses, which is outside the scope of our study. To account for uncertainties in topology and branch lengths, the posterior distribution of trees produced in the dating analyses was sampled in the MCMC chains of the biogeographical analyses (363 trees after resampling at a frequency of 600000). *Salticus scenicus* was pruned from the trees since it is a single representative of a diverse distant outgroup and its inclusion could bias the analyses (Mooers and Schluter, 1999).

The strength of evidence in favor of each hypothesis was compared through Bayes factors, with marginal likelihoods estimated with stepping-stone analysis (Xie et al., 2011) with 25 steps, each step with a burn in of 10000, 10,000 post-burn in generations and sampling frequency of 100. After selecting the most supported candidate hypothesis, we performed a MCMC run with 1,000,000 simulations, logging states every 1000. Mixing of the MCMC run was assessed with Tracer 1.7.1. The maximum clade credibility tree was summarized with the maximum a posteriori marginal probability of ancestral areas. Scripts used are available at https://doi.org/10.5061/dryad.7wm37pw11.

3. Results

3.1. Data

We recovered a total of 1947 UCEs present in at least four terminals, with an average of 724 UCEs per specimen (standard deviation 226.67; minimum 377 except *Havaika* sp. [Kauai, d300], with only 25 UCEs). The mean UCE alignment length was 652 bp (minimum 209, maximum 1416 bp). The 50 % occupancy matrix (UCEs50p), used in the primary analyses, contained 193 UCEs whose mean aligned length was 762 bp (min. 340; max. 1316; 95 % CI ± 28.5). The 33 % occupancy matrix had 1229 UCEs, and the 85 % occupancy matrix had 30 UCEs. The total length of the concatenated UCEs50p alignment was 147,234 bp. The concatenated UCEs50p dataset has approximately 44 % missing data. The number of taxa with successful bycatch data was 26, 47 and 39 for the 16SND1, 28S and COI, respectively. The total length of the 28S_16SND1_COI matrix was 2,434 bp with 34 % missing data. The mitochondrial loci alignment has a total of 12,466 bp with 60 % missing data. Raw reads are deposited in SRA under the BioProject number PRJNA1076327 and matrices are available at https://doi.org/10.5061/dryad.7wm37pw11.

3.2. Phylogenetic relationships

The UCE results (Fig. 1) resolve major aspects of harmochirine phylogeny with strong support, including (1) the monophyly of the subtribe, (2) its basal separation into two clades here called Harmochirita and Pellenita (see 5. Taxonomy, below), and (3) the isolation of *Neaetha* as the sister group to the remaining pellenites. Each of these results is supported by 100 % values in assessments by standard bootstrap, approximate LRT, and ultrafast bootstrap, and the results hold for datasets of different occupancies (33p, 50p, 85p) and for the ASTRAL analysis (see Supplementary Material Files S2 – S6 and tree files on https://doi.org/10.5061/dryad.7wm37pw11 for further details on alternative analyses). Although some nodes in the ASTRAL analyses show relatively low gene tree concordance (first quartet < 50 %), the local posterior probabilities (which accounts for discordance) show higher values, suggesting that the discordance is not enough to discredit the nodes. The relatively low concordance between genes might nevertheless explain some differences between results. *Modunda* for the first time is placed phylogenetically, as a member of the Harmochirita. Among the Pellenita, a clade of four genera is resolved: *Havaika*, *Hivanua*, *Pellenattus*, and *Habronattus*. The first two of these are from Pacific Islands; the last two from the Americas. This clade will be referred to as the America-Pacific clade. Almost all other harmochirines are from Africa and Eurasia.

The results reveal that generic limits need to be adjusted to maintain monophyly. The monophyly of a core of *Pellenes* species is well supported, but several species are placed elsewhere. The species previously known as *Pellenes stepposus* is placed among the harmochirites and *P. bulawayoensis* with *Neaetha*. As noted under section 5. Taxonomy, below, this requires that these species be moved to the genera *Sibianor* and *Neaetha*, respectively. Also, the American *Pellenattus*, which has been considered a subgenus of *Pellenes*, is more closely related to *Habronattus*, requiring that it be considered an independent genus. The harmochirines of the Marquesas Islands, formerly placed in *Havaika* and *Habronattus*, are in fact more closely related to *Pellenattus*, and are therefore described as the new genus *Hivanua* by Maddison (2024). Otherwise, the genus *Habronattus* is well supported as monophyletic for the first time. Previous transcriptome-based phylogenomic results have suggested that the AAT clade of *Habronattus* (see Fig. 1) may be more

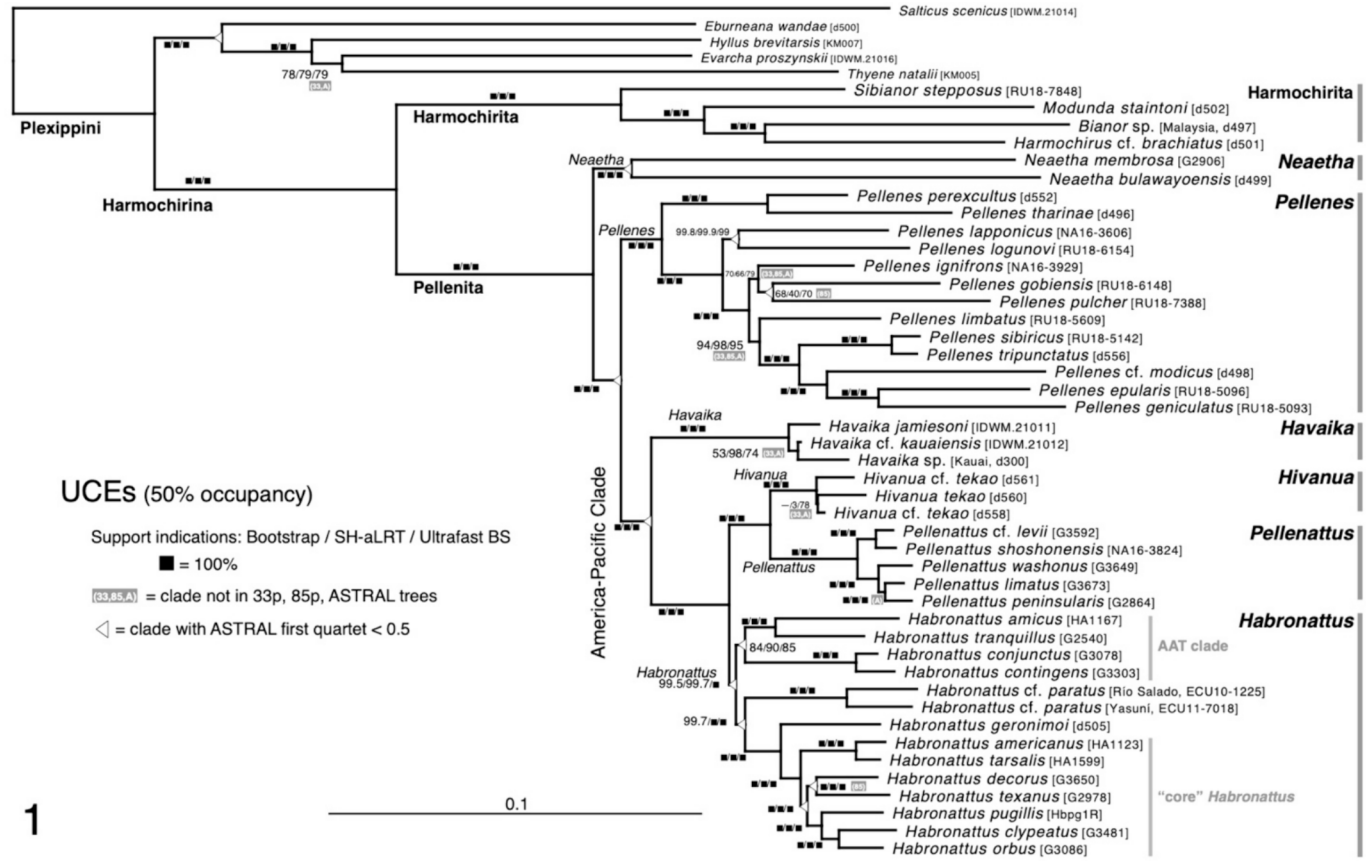

Fig. 1. Summary of UCE phylogenetic analyses. Maximum likelihood tree (IQ-TREE) from 193 UCE loci with at least 50 % occupancy (UCEs50p concatenated matrix). Branches marked with support values: standard bootstrap percentage / approximate LRT test / ultrafast bootstrap percentage (percentage replaced by black square if 100 %). Clades also appear in analyses from different numbers of loci (33 % occupancy — 1229 loci; 85 % — 30 loci) and ASTRAL, except where noted. Triangles show clades with a higher frequency of discordant topologies in the ASTRAL analysis.

closely related to *Pellenattus* than to the remaining *Habronattus* (Leduc-Robert and Maddison, 2018), but the much denser sampling of *Habronattus* relatives in this study supports the genus as monophyletic, although with a stem branch that is very short and has indications of discordant gene tree topologies (Fig. 1, Supplemental Material Files S5, S6). Another possible taxonomic act would be to transfer *Pellenes* (*Pellenatus)* species to *Habronattus*, but that would also require the transfer of the recently described genus *Hivanua* to *Habronattus*. Given that *Habronattus* is already a very large genus, and the three taxa have very distinctive morphology, ecology and behavior, we prefer to raise the subgenus *Pellenattus* to generic status. Relationships within *Habronattus* are concordant with those of Leduc-Robert and Maddison (2018). Notably, the UCE data confirm the placement, previously based only on mitochondrial DNA, of the *H. paratus* group as sister to the large clade spanning from the *H. dorotheae* group to the *H. coecatus* group. The sister group of *Habronattus* is resolved as the clade consisting of *Hivanua* and *Pellenattus*.

Analysis of partial mitochondrial genomes recovered as bycatch show results that are largely concordant with the UCE loci (Fig. 2). The most notable differences concern *Neaetha*, which falls as paraphyletic, and *Habronattus*, which is shattered into three pieces, though with low bootstrap support. As mentioned above, incomplete lineage sorting might be responsible for the differences, since those nodes show lower levels of gene tree concordance.

The legacy loci 28S, 16SND1, and COI (Fig. 3) place the Sanger-sequenced species of *Sibianor* (shown in bold) with *S. stepposus* with high bootstrap support not only in the constrained analysis (Fig. 3) but also in the unconstrained IQ-TREE analysis (bootstrap 99.8 %). This confirms the placement of "*Pellenes*" *stepposus* in *Sibianor*. The Sanger-sequenced species of *Bianor*, *Pellenes*, and *Havaika* are placed with their expected UCE-sequenced relatives.

The phylogenetic trees in the divergence dating and biogeographical analyses differ from that of Fig. 1 in having *Neaetha* paraphyletic. The divergence dating tree also differs in placing *Pellenes perexcultus* and *P. tharinae* as sister to the America-Pacific clade. Nevertheless, there is strong support in the full analysis of 193 loci for the monophyly of both *Neaetha* and *Pellenes*. The differences in the topology could have been caused by stochasticity of gene sampling in a reduced matrix, uneven taxon sampling across clades (violating the tree model used in StarBeast), and /or missing data in the 80 % matrix.

The taxonomic changes following from these phylogenetic results are presented after the Discussion, including the formal proposal of two infratribes (the Pellenita, formerly the "pellenines", and the Harmochirita, formerly the harmochirines s. str.), and the transfer of species to *Sibianor*, *Neaetha*, and *Pellenattus*.

3.3. Divergence dates and molecular clock rates

The first divergence in the sampled Harmochirina clade is estimated in the Miocene, about 14 mya (median = 14.55, 95 % HPD = [12.78, 17.22]; Fig. 4). The America-Pacific clade is estimated to have started to diversify at the Miocene to Pliocene boundary, around 5.3 mya (median = 5.31, 95 % HPD = [4.52, 6.30]). The clade formed by *Pellenattus* plus *Hivanua* is estimated to be approximately 2.3 my (median = 2.35, 95 % HPD = [1.77, 2.97]). *Habronattus* started to diversify around 4 mya (median = 3.96, 95 % HPD = [3.45, 4.87]. As noted above, the maximum clade credibility tree topology of the dating analysis differs in a few branches from the topology obtained with other methods (Fig. 1

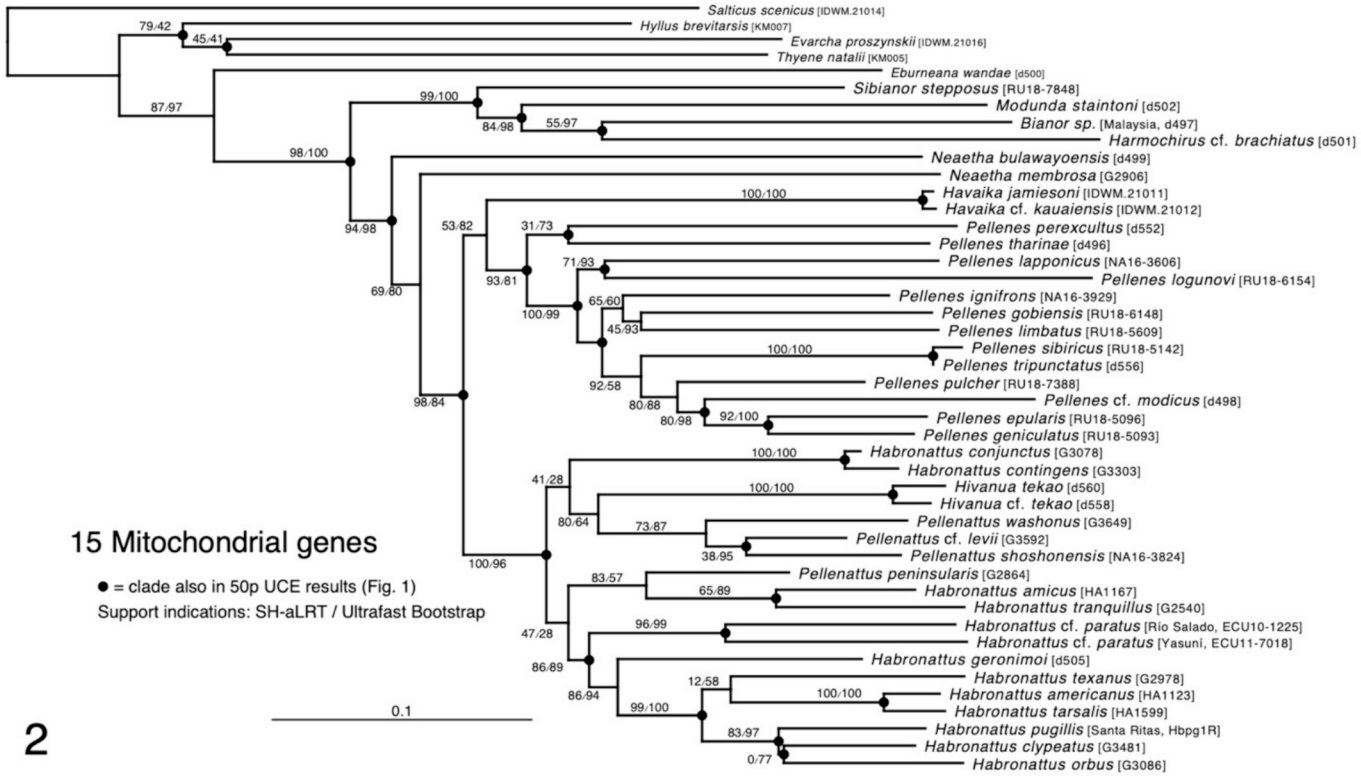

Fig. 2. Maximum likelihood tree (IQ-TREE) from 15 mitochondrial loci (average 5270 bp per taxon), including protein-coding and rRNA genes. Branches marked with approximate LRT test / ultrafast bootstrap percentage. Filled circles show agreement between this tree and the UCE tree from nuclear loci.

vs. 4, position of *Pellenes perexcultus* and *P. tharinae*), but these differences likely do not influence our clade ages and biogeographic conclusions since we incorporated topology uncertainty in these analyses. The results without island calibrations showed no difference in the posterior distribution of ages and rates (input files and results at https://doi.org/10.5061/dryad.7wm37pw11), and the run under prior show a different posterior distribution, meaning that the island age calibration is not influencing the results and that the molecular data is driving the posterior ages and rates.

The rate of molecular evolution for COI was estimated to be 0.0188 substitution per million years, with the 95 % high posterior density interval between 0.0152 and 0.0228 (mean = 0.0188, SD = 0.00193). The 28S rate was estimated to be 0.00141 (95 % HPD = [0.0010, 0.0017]). UCE clock rates are estimated to be slower than the COI but faster than the 28S, with the exception of UCE-2003510, which was the gene region with the lowest rate (0.00074 substitution per million years; Supplemental Material File S7, S8). The average rate for all UCEs is estimated to be 0.00658 substitutions per million years (standard deviation = 0.00385, 95 % HPD = [0.0018, 0.0134]). All UCEs used for dating were confirmed as coding regions. Summary statistics for the clock rates as well as UCE annotations can be found in the Supplementary Material File S8.

3.4. Biogeography

The rjMCMC shows no support for a model that includes the J parameter (P(DEC) = 0.51; P(DEC + J) = 0.49). Even though the difference between the model probabilities is low, it is more parsimonious to use a model with fewer parameters; we also note the problems associated with the J parameter mentioned previously (2.7. Biogeographic Analyses). Bayes factor analysis suggests that there is strong evidence favoring H1 over other hypotheses (Table 1, Fig. 5). This suggests that the best explanation for the biogeographic distribution of harmochirine genera are two independent dispersals to the Pacific from the Americas, and that American taxa came from Eurasia. Fig. 5 summarizes posterior probabilities for ancestral ranges according to H1. The MRCA of Harmochirina was most likely distributed in Africa, and of the Harmochirita in Eurasia (we note, however, that African harmochirites, of which there are many, were not included in the analysis). The ancestral ranges of the basal nodes of the pellenites are not confidently estimated, while the ancestral range of the America-Pacific clade was most likely in the Americas only, and dispersed to Hawaii between 5.3 and 0.014 mya, after the first speciation event that originated the branch leading to *Havaika*. Our data does not allow us to distinguish clearly whether the ancestral area of the *Pellenattus* plus *Hivanua* clade was in the Americas only, or in both Americas and Marquesas Island. The dispersal to the Marquesas could have happened between 4.15 and 2.35 mya.

4. Discussion

4.1. Phylogeny

With much denser sampling of taxa from outside the Americas and a larger number of loci, our results confirm the basic division of harmochirines into two subgroups, and for the first time resolve the phylogeny of the Pellenita. *Neaetha* is the sister group to the remaining pellenites, and *Pellenes* is the sister to a clade of four genera from the Americas and the Pacific Islands. These results now allow us to consider divergence times, biogeography, and evolutionary patterns within the America-Pacific clade.

4.2. Divergence times and molecular clock

The lack of fossil (and/or clear geological information) hampers divergence time estimation and may consequently hinder our understanding of evolutionary processes in diverse and recent groups, such as in *Habronattus* and *Pellenattus*. In such cases, divergence dating relies on

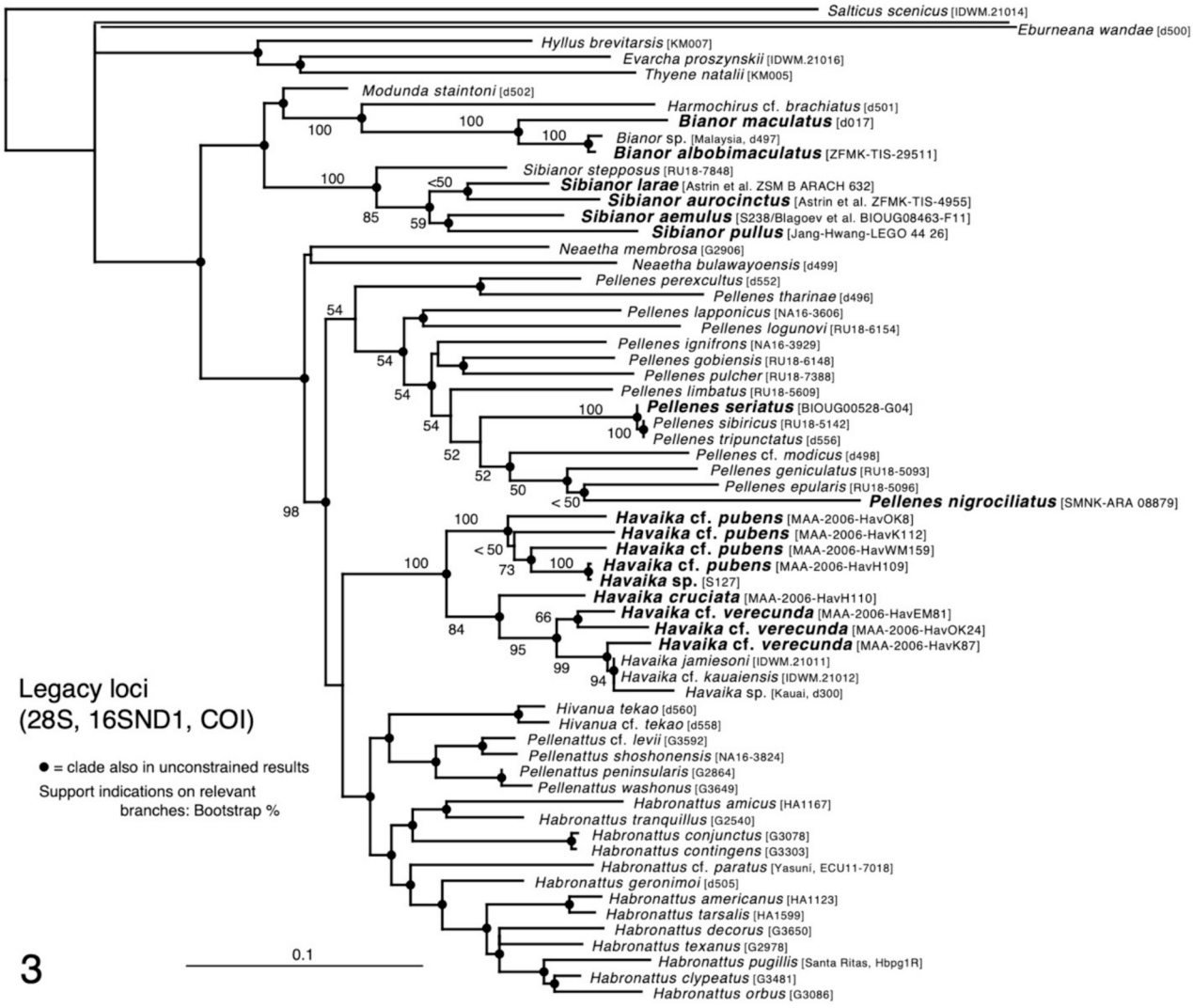

Fig. 3. Maximum likelihood phylogenetic tree from concatenated 28S, 16SND1, and COI data, combining taxa known only from Sanger sequencing of those loci (in **bold**) with UCE taxa (not in bold) from which bycatch data was obtained from those same loci. Tree inferred by RAxML with skeletal constraints to force relationships among UCE taxa to match Fig. 1. Standard bootstrap percentages shown only in the vicinity of Sanger-sequenced taxa, because those are the only free to move in the analysis. Filled circles show clades also appearing in unconstrained IQ-TREE analysis. *Eburneana* on long branch, cut and overlapped to reduce length.

secondary calibrations (e.g., Hedin et al., 2020) or molecular clock rates estimated for other taxa (e.g., Monjaraz-Ruedas et al., 2023). The former option, although useful, may infer inaccurate dates, and the latter will only be reliable if the clock rate is similar between the taxa of interest (Schenk, 2016; Tao et al., 2020). In fact, our molecular rate estimation based on fossil and geological information suggests that COI and 28S rates are considerably higher in harmochirines (and maybe all salticids) as compared to distantly related dysderid spiders (Bidegaray-Batista and Arnedo, 2011). Contrasting with dysderids, salticids are diurnal, active hunters, with short generation times, perhaps explaining the higher substitutions rates found here. Our estimated COI and 28S rates are more similar to those of lycosoid spiders (Piacentini and Ramírez, 2019), which belong to the RTA (Retrolateral Tibial Apophysis) clade together with salticids. Therefore, the higher rates could be general for RTA families and the rates estimated here provide a reasonable prior for studies of RTA clade taxa with little or no fossil information, especially for jumping spiders. It is also worth noting that differences in rates could be related to the model used here, the multispecies coalescent, in contrast to the concatenation approach used in previous studies. Concatenation can inflate the tree length and underestimate rates (Ogilvie et al., 2017). The rates estimated here could be more accurate than previously estimated rates for spiders in general. Our understanding of molecular evolution in Araneae could benefit from studies using multispecies coalescent dating with other spider taxa.

We also provide for the first time an estimation of molecular clock rates for a small subset of UCEs in spiders. UCEs have been useful for studies at different phylogenetic depths, including at the species and population levels (Starrett et al., 2017; Azevedo et al., 2023; Newton et al., 2023). At these shallow levels, fossil information is usually unavailable, and, therefore, a UCE rate is informative for evolutionary studies. Researchers could use the rate statistics provided here (Supplementary Material File S7, S8) to inform a prior distribution for each specific UCE locus, or as a more general prior using the average and standard deviation (or the 95 % posterior density interval) across all UCEs. It is worth noting that the UCEs used here are in a high occupancy matrix (85 %), which might indicate that these loci are more conserved. Consequently, the rates might be biased towards lower rates, and care must be taken when generalizing to all UCEs, specially for non-coding UCEs. Researchers should also pay attention to the flanking regions of UCE alignments to make sure they do not contain extensive regions of indels and low sequence identity before using the rates here as priors. Extremely variable flanking regions may suggest non-coding sites with

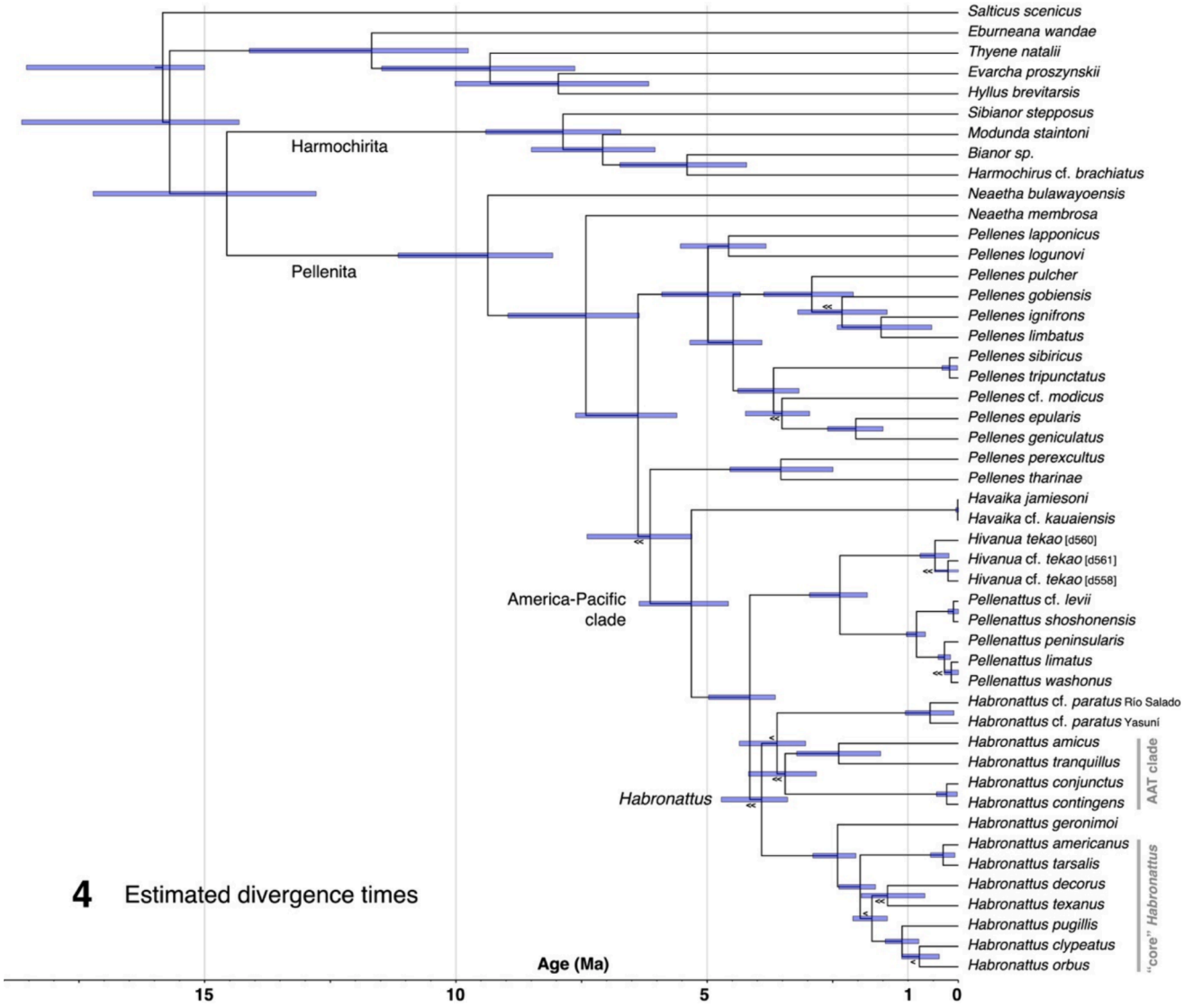

Fig. 4. Estimated divergence times inferred by StarBeast3 from 32 loci (85 % occupancy UCEs + COI + 28S), with time calibrations from amber fossils and geological age of islands. Bars on phylogeny show HPD credibility intervals for node ages. Nodes have posterior probabilities greater than 0.95 except those marked with < (0.90 to 0.95) and with ≪ (less than 0.90).

faster evolutionary rates. In these cases, less informative prior distributions that allow rates to be faster than estimated here can be used (the same care should apply to 28S loop regions, also trimmed here). Lastly, since all UCEs used here for the dating analysis are from coding regions, this general UCE rate might also be (carefully and thoughtfully) extrapolated to inform prior distributions on transcriptome data for RTA Clade families.

Our divergence dates agree generally with previous studies (Bodner and Maddison, 2012), showing that the Harmochirina spiders started to diversify during the mid Miocene (around 15 Mya; Fig. 4). Impressively, the diversity found in *Habronattus* is a result of a very young process of diversification that is estimated as not older than 5 million years old. In particular, the clade labeled "core" *Habronattus* in Fig. 4, with the highest species and ornamental diversity in the genus, is perhaps younger than 2.5 Mya. Since most of the morphological and behavioral diversity is associated with courtship, sexual selection (perhaps combined with introgression) may have played an important role in the rapid radiation of paradise jumping spiders, as suggested originally by Masta and Maddison (2002). The dates and molecular rates provided here will be an important source of information for testing hypotheses of diversification in *Habronattus* and help us better understand processes related to sexual selection and to the evolution of mating traits and courtship behavior.

4.3. Biogeography

Previous authors have suggested that *Habronattus* represents a transcontinental dispersal from Eurasia (Bodner and Maddison, 2012; Hill and Edwards, 2013). Here we corroborate this Eurasian origin, and we show that in fact, the colonization is older than the genus *Habronattus* and happened around 5 Mya in the MRCA of the America-Pacific clade (Fig. 5). Warmer climates during the Pliocene (5.3 to 2.58 Mya) may have facilitated dispersal through the Bering Strait and adjacent areas (Rybczynski et al., 2013). Although a more southern transpacific dispersal through ballooning is possible, our analyses suggest that the Pacific Islands of Hawaii and the Marquesas did not serve as stepping stones for arrival in the Americas, or for each other. Our results instead indicate that *Havaika* and *Hivanua* represent two independent dispersal events to the Pacific Islands from the Americas (Fig. 5). Colonization of different Pacific Islands independently from the mainland has also been suggested for long-jawed tetragnathid spiders, crab spiders and Asteraceae plants (Gillespie, 2002; Arnedo and Gillespie, 2006; Garb and

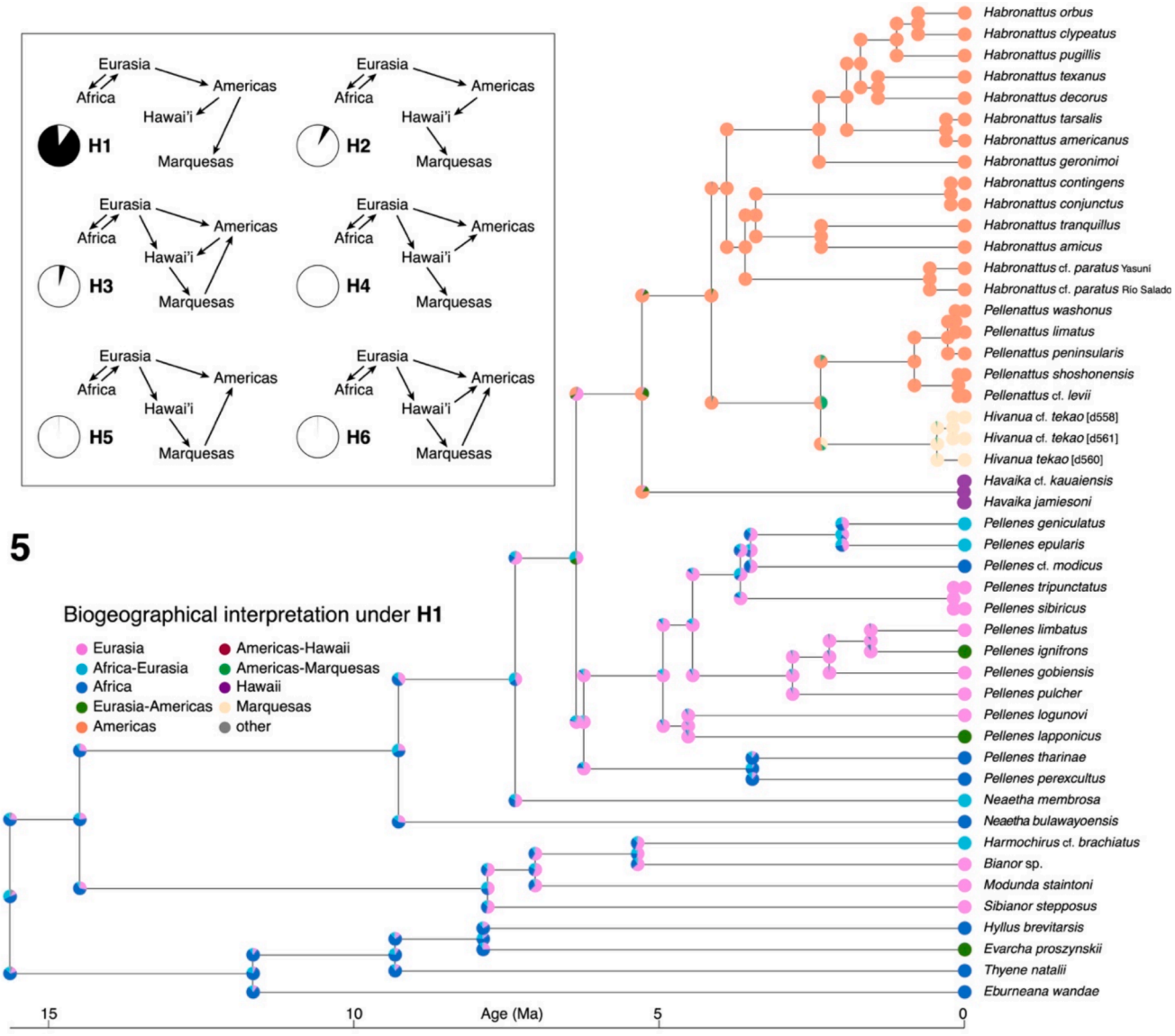

Fig. 5. Biogeographical history inferred by RevBayes using the DEC model, based on posterior distribution of trees from the dating analysis and summarized on the maximum clade credibility tree. Inset shows six dispersal constraint hypotheses tested (H0 = unconstrained dispersal); black pie slice for each shows relative marginal likelihood of hypothesis. Main figure shows inferred ancestral ranges under the assumption of dispersal constraint H1. Pies show posterior probabilities of alternative ranges at each node.

Table 1
Marginal likelihoods and Bayes factor (BF) relative to the best biogeographic model (H1).

Scenario	Marginal Likelihood	BF relative to h1
H1	−56.34173	-
H2	−59.22177	2.88004
H3	−59.30841	2.96668
H0	−60.89613	4.5544
H6	−62.83803	6.4963
H5	−62.98513	6.6434
H4	−70.04974	13.70801

Gillespie, 2006; Knope et al., 2020). This is not a universal pattern: studies in other animals and plants suggest that many Marquesan species may have arrived from the west (Australasian) or by island hopping from Hawaii (Gillespie et al., 2008; Hembry, 2018). Whether generalizations can be made about dispersal patterns will have to await better-resolved phylogenies becoming available for more Pacific Island taxa.

Harmochirines might have had a special advantage in colonizing young volcanic islands, as the group in general is found on open, sparsely-vegetated ground that is often sunny, and relatively hot. Notable exceptions are *Havaika* and *Hivanua* themselves, which appear to be foliage dwellers (Maddison, 2024), but their shift in habitat may have occurred post-dispersal as the islands became vegetated.

4.4. Evolution of sexual traits

Habronattus, remarkable for its elaborate courtship ornaments and behaviours (Peckham and Peckham, 1889, 1890; Elias et al., 2003, 2012; Rivera et al., 2021), stands out among the harmochirines. No particular suite of ornaments or courtship behaviours is known that could be considered a synapomorphy of *Habronattus*, because they are so variable in their details. One might claim a shared tendency, i.e., a hidden synapomorphy, of a mechanism promoting complexity in *Habronattus*. However, the placement of the *Habronattus paratus* and *H. dorotheae* species groups (the latter represented here by *H. geronimoi*) suggests that any such mechanism might have arisen twice, once in the

AAT clade and once in the "core" *Habronattus* (Fig. 1). In the AAT clade, the sweeping and intricate fringes of the first leg seen in *H. tranquillus* and *H. hirsutus* exceed in complexity any ornaments among the harmochrines outside *Habronattus*. In the "core" *Habronattus*, complex ornamentation is well represented. However, between this ornamented clade and the AAT clade lie the *dorotheae* group and the *paratus* group. Members of these latter groups resemble *Pellenes*, and comfortably match the modesty of other pellenites. Their males do have ornamentation, but only to the extent of most salticids, e.g., a slightly fringed first leg, perhaps (e.g. *H. geronimoi*) with darkness of brown varying from one leg segment to another. Indeed, *H. paratus* was not thought to be a *Habronattus* by Griswold (1987) based on its resemblance to *Pellenes*, in particular in its long first legs.

One phylogenetically-scattered ornament, possibly tied to a unique visual system (Zurek et al., 2015), is a clypeus (face) covered with red scales. Bright red courtship ornaments are well known in *Habronattus*, from red palps and legs (e.g., *H. americanus;* Bougie et al., 2024) to red faces (e.g., *H. coecatus* and at least 5 of its close relatives, as well as *H. hirsutus*, *H. ocala*, *H. luminosus*; Taylor and McGraw, 2013). Zurek et al. (2015) found a ruby-coloured filter in the anterior median eyes that appears to provide *Habronattus* the ability to distinguish red from green, an ability likely lacking in most salticids. Indeed, red courtship ornaments are rare in salticids except in a few notable clades, *Habronattus* being one of them. Although otherwise with muted colours and ornaments, other pellenites have bright red faces. Several species of *Pellenes* are distinctive for their red male faces, such as *P. ignifrons*, *P. seriatus*, and *P. tripuncatus*. *Pellenattus* males often have a modestly red face, and it is bright red in an undescribed species near *P. levii* from California. These observations of red faces outside *Habronattus* hint to the breadth of the distribution of the ruby filter in their eyes, if those red faces were selected by females with a red-distinguishing filter. The phylogeny would lead us to predict that such a filter occurs throughout the clade of *Pellenes, Habronattus*, *Pellenattus*, *Havaika*, and *Hivanua*.

In addition to behaviour and ornaments, sexual traits in spiders include the genitalia, the male palp and female epigyne. Fig. 6 shows the phylogeny of pellenites with diagrams of the parts of the male palp that inject sperm into the female (embolus, shown in red) or that accompany them (terminal apophysis, "TmA", shown in blue). The phylogenetic results help us understand the gains and losses of the TmA, and its changes in form. The harmochirites lack a TmA and thus resemble *Neaetha*. The TmA is restricted to *Pellenes* + American-Pacific clade members. We favour a scenario of TmA homology with secondary losses (in America-Pacific clade) because of an expectation that loss may be easier than gain. However, simply counting changes, it would be equally parsimonious to assume multiple origins, depending on interrelationships within *Pellenattus*. Regarding the form of the TmA, *Habronattus* had been thought unique among harmochirines in having an elbowed TmA, but Maddison (2024) reports an elbow in *Hivanua tekao* as well. That leads to an ambiguity: either the MRCA of the *Habronattus-Hivanua-Pellenattus* had an elbowed TmA which was lost subsequently in *Pellenattus* and some *Hivanua*, or it is convergent in *Habronattus* and *Hivanua*. Changes in the form of the TmA are more simply characterized within

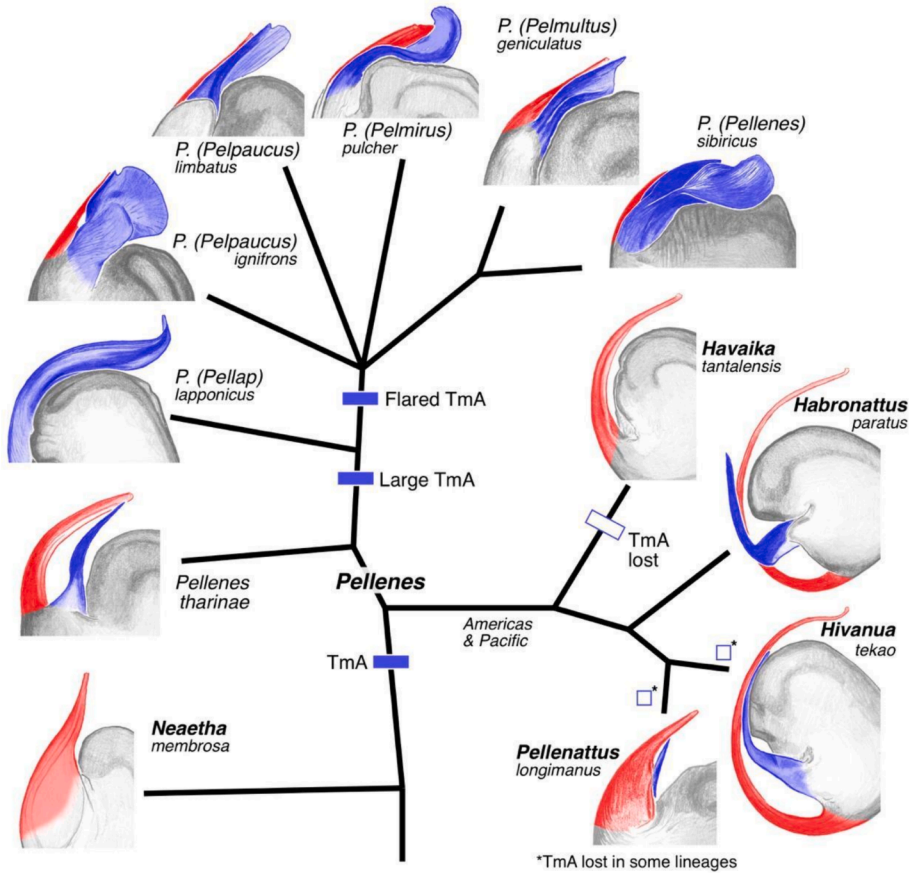

Fig. 6. Evolution of the male embolic division in the infratribe Pellenita, displayed on the UCE phylogeny. Shown is the terminal portion of the male palp's bulb, left palp, ventral view. Embolus shown red; terminal apophysis (TmA) blue. The (red) embolus of *Pellenes* (*Pellap*) is hidden behind the larger TmA, and thus not visible in this ventral view. "Flared" refers to the widening of the tip of the TmA. Although a single origin of the TmA is indicated, equally parsimonious (assuming gains of TmA are as simple as losses) would be two origins, one in *Pellenes* and one in the clade of *Habronattus*, *Hivanua*, and *Pellenattus*. The sister group, infratribe Harmochirita, has an embolic division similar to that of *Neaetha*. (Note, the choice of colours does not imply a functional connection to the coloured structures in Fig. 7; i.e. the red embolus does not engage with the red coupling pocket.) ©2024 W. Maddison, under a Creative Commons CC BY-4.0 license. (For interpretation of the references to colour in this figure legend, the reader is referred to the web version of this article.)

Pellenes, based on the phylogeny (Fig. 6): initially small and thin like those in the America-Pacific clade, expanded considerably in size to be larger than the embolus in both width and length ("Large TmA" in Fig. 6). Subsequently the tip of the TmA widened ("flared"), which is thus a synapomorphy for all described subgenera of *Pellenes* except for *Pellap*.

The female epigyne, a sclerotized plate which bears the genital openings (Fig. 7), shows a diversity of unusual and derived forms in most subgenera of *Pellenes*, but in others has a form similar to that of harmochirites — a central coupling pocket flanked by two crescent-shaped ridges framing the atria and copulatory openings. An epigyne very similar to the harmochirite form is seen in the inexcultus group of *Pellenes* (here represented by *Pellenes tharinae* and *P. perexcultus*), and in *Havaika, Hivanua* and *Habronattus*. This arrangement of a pocket with two big crescents can be parsimoniously considered ancestral for the pellenites. These crescent-shaped atrial ridges appear to have been reduced similarly in *Pellenes*, *Neaetha*, and in *Pellenattus*: in each, the length of the ridge bounding the copulatory opening was shortened, and the opening shifted toward the posterior, near the back of the coupling pocket. However, *Pellenes* epigynes are so seriously modified that their homologies are unclear. In *P. tripunctatus*, a broad shallow pocket at the extreme anterior appears to be homologous to the coupling pocket by position, but that is uncertain because the relationship to other parts is so modified. *Pellenes ignifrons* appears to have no coupling pocket at all, but whether it might have disappeared to the front (i.e., *P. tripuncatus*'s anterior extension taken even further) or to the back is unclear. *P. pulcher* appears to have big crescent shaped ridges, but a small opening at their posterior end could be the primary opening instead, and the crescents, much more delicate than typical, could be merely exaggerated folds inside the atrium as seen in, for example, *Havaika*. Regardless, the phylogeny reveals that the strong modification of the atrial ridges is a synapomorphy of a major clade within *Pellenes*.

5. Taxonomy

5.1. Subtribe Harmochirina Simon, 1903

The two subgroups of harmochirines (referred to as harmochirines s. str. and pellenines by Maddison, 2015) are here established formally as infratribes to be able to refer to each separately. There is no standard suffix for infratribes; a suffix with "t" is used so as to make the adjectival forms for the infratribe and subtribe distinct, "harmochirite" and "harmochirine" respectively.

Excluded from the genera listed by Maddison (2015) as harmochirines are *Eburneana*, which the phylogenetic results place outside the subtribe (Fig. 1), and *Iranattus* (=*Monomotapa*), which is also outside the subtribe according to a recent study (Marathe et al., 2024).

5.1.1. Infratribe Harmochirita Simon, 1903, new status

Genera included:
Bianor Peckham & Peckham, 1886.
Harmochirus Simon, 1885.
Microbianor Logunov, 2000.
Modunda Simon, 1901.

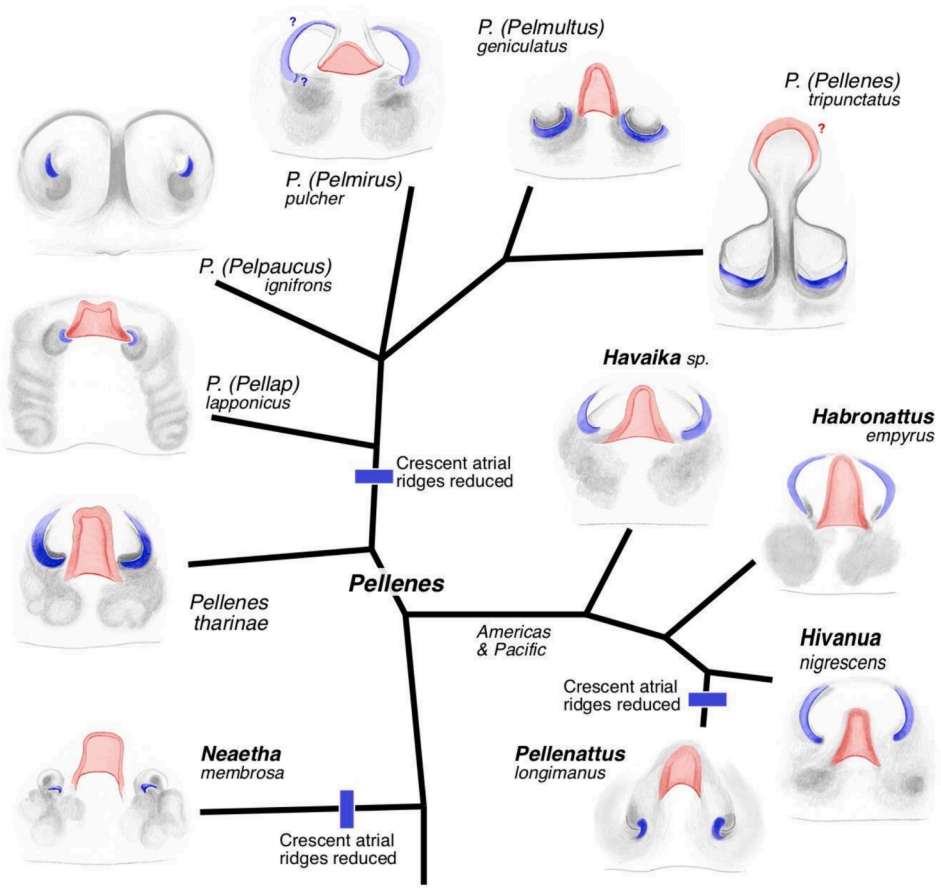

Fig. 7. Evolution of the female epigyne in the infratribe Pellenita, displayed on the UCE phylogeny. Central coupling pocket shown in red; ridges forming the boundary of the copulatory openings shown in blue. The homologies are unclear in *P. tripunctatus* and *P. pulcher*. The sister group, infratribe Harmochirita, has an epigyne similar to that of *Pellenes tharinae*, *Havaika*, *Habronattus*, and *Hivanua*. (Note, the choice of colours does not imply a functional connection to the coloured structures in Fig. 6; i.e. the red coupling pocket does not engage with the red embolus.) (For interpretation of the references to colour in this figure legend, the reader is referred to the web version of this article.)

Napoca Simon, 1901.
Sibianor Logunov, 2001.

The molecular placement of the elongate-bodied *Modunda* among harmochirites is surprising, given that it is nestled among compact-bodied and slightly beetle-like genera. The data confirm Logunov's (2001) distinction of *Sibianor* from *Bianor* and *Harmochirus*. The harmochirites include the well-known genera *Bianor*, *Harmochirus*, and *Sibianor*, as well as a few others that were not included in the analyses here but are assumed to belong to the infratribe based on morphological data from previous studies (Logunov, 2001; Maddison, 2015).

5.1.1.1. Genus Sibianor Logunov, 2001. Sibianor stepposus (Logunov, 1991), **comb. nov.** — Logunov's original placement in *Bianor* (from which *Sibianor* was later split) was in fact correct according to the molecular data (Figs. 1, 3). This placement is consistent with its proximal tegular lobe (seen in *Sibianor* but none of the pellenites), and the lack of a terminal apophysis accompanying the embolus (all *Pellenes* have a TmA). The species also has the classic appearance of *Sibianor*: compact, shiny, with swollen first patella and tibia in the male.

5.1.2. Infratribe Pellenita Petrunkevitch, 1928, new status
Genera included:
Habronattus F.O. Pickard-Cambridge, 1901.
Havaika Prószyński, 2002.
Hivanua Maddison, 2024.
Neaetha Simon, 1884.
Paraneaetha Denis, 1947.
Pellenattus Maddison, 2017.
Pellenes Simon, 1876.
Pellolessertia Strand, 1929.

The resolution of pellenite phylogeny (Fig. 1) requires a revision of the limits of *Pellenes* and other genera. *Havaika* and *Hivanua* are discussed by Maddison (2024), and *Habronattus* has been discussed elsewhere (Griswold, 1987; Maddison and Hedin, 2003; Maddison, 2017; Leduc-Robert and Maddison, 2018); we here focus on *Neaetha* and *Pellenes sensu lato*. Other genera not included in our analyses are assumed to belong to the infratribe based on morphological data from previous studies (Logunov, 2001; Maddison, 2015).

5.1.2.1. Genus Neaetha Simon, 1885. Neaetha bulawayoensis (Wesołowska, 1999), **comb. nov.** — The phylogenomic placement of this species with *Neaetha membrosa* might seem to contradict the reported presence of a TmA (Wesołowska, 1999), but re-examination shows that *N. bulawayoensis* in fact lacks a terminal apophysis. We therefore transfer the species to *Neaetha*, as the phylogeny requires.

5.1.2.2. Genus Pellenes Simon, 1876. Despite its great diversity of forms of genitalia and bodies, *Pellenes* is recovered strongly as monophyletic, once *Pellenattus* is removed. Thus, except for two Holarctic species (*P. lapponicus* and *P. ignifrons*) that have likely only recently arrived to the Americas, the genus is Afro-Eurasian (with a few Australasian species).

5.1.2.3. Genus Pellenattus Maddison, 2017, ***new status.*** The placement of *Pellenattus* as more closely related to *Hivanua* and *Habronattus* than to *Pellenes* (type species *P. tripunctatus*) requires it be split off from the latter. We here raise *Pellenattus* to the status of a separate genus. Although this result is clear from the phylogenomic data, and makes sense geographically (given that *Pellenattus*, like *Habronattus*, is restricted to the Americas), it suggests convergence or reversals in a few morphological traits. *Pellenattus* shares with some Eurasian *Pellenes* the loss of simple large crescent-shaped atria of the epigynum, and a clear and narrow set of chevrons on the abdomen.

The following species are therefore transferred to the genus *Pellenattus*:

Pellenattus apacheus (Lowrie & Gertsch, 1955), **comb. n.**
Pellenattus canadensis (Maddison, 2017), **comb. n.**
Pellenattus cinctipes (Banks, 1898), **comb. n.**
Pellenattus corticolens (Chamberlin, 1924), **comb. n.**
Pellenattus crandalli (Lowrie & Gertsch, 1955), **comb. n.**
Pellenattus grammaticus (Chamberlin, 1925), **comb. n.**
Pellenattus levii (Lowrie & Gertsch, 1955), **comb. n.**
Pellenattus limatus (Peckham & Peckham, 1901), **comb. n.**
Pellenattus longimanus (Emerton, 1913), **comb. n.**
Pellenattus peninsularis (Emerton, 1925), **comb. n.**
Pellenattus shoshonensis (Gertsch, 1934), **comb. n.**
Pellenattus washonus (Lowrie & Gertsch, 1955), **comb. n.**

Declaration of competing interest

The authors declare that they have no known competing financial interests or personal relationships that could have appeared to influence the work reported in this paper.

CRediT authorship contribution statement

Guilherme H.F. Azevedo: Writing – review & editing, Writing – original draft, Visualization, Investigation, Data curation, Conceptualization. **Marshal Hedin:** Writing – review & editing, Supervision, Resources, Project administration, Funding acquisition, Data curation, Conceptualization. **Wayne P. Maddison:** Writing – review & editing, Writing – original draft, Visualization, Validation, Supervision, Resources, Project administration, Investigation, Funding acquisition, Formal analysis, Data curation, Conceptualization.

Data availability

The link to the repository with the data is in the main manuscript file. and will be released after publication of the manuscript.

Acknowledgements

This work would not have been possible without those assisted with taxon sampling, without whom this work would not have been possible. Indeed, the project began because Galina Azarkina greatly facilitated field work in southern Siberia that yielded a broad sample of *Pellenes*, including species groups not otherwise available. She supplied as well specimens of *P. epularis* and *P. geniculatus*. Critical specimens were also supplied by Charles Haddad (*Pellenes* spp., *Neaetha bulawayoensis*), Marnix Bos (*Neaetha membrosa*), Pir Asmat Ali (*Modunda staintoni*), Karl Magnacca (*Havaika* spp.), Miquel Arnedo and Rosemary Gillespie (*Hivanua* spp.), and Liza Fowler (*Pellenes perexcultus*). Members of *Habronattus* collecting teams included Tierney Bougie, Samuel Brown, Ben Coulter, Damian Elias, Dariana Guerrero, Colin Hutton, Michael Lowder, Julia Soares Parreiras, Pierre Paquin, Victoria Rayno, Andrew Rivera, Karina Silvestre, and Patrick Zephyr. We offer our deep thanks to these colleagues. We also thank Kiran Marathe for assistance with lab work to obtain sequences for *Hyllus brevitarsis* and *Thyene natallii*. GHFA and research at San Diego State University was supported by NSF DEB 1754591to MH; research at the University of British Columbia was supported by an NSERC Discovery Grant to WPM. San Diego State University stands upon land that carries the footsteps of millennia of Kumeyaay people. The Associate Editor and anonymous reviewers provided comments that helped to strengthen the manuscript. Rodrigo Monjaraz-Ruedas helped running additional analyses.

Appendix A. Supplementary material

Supplementary data to this article can be found online at https://doi.org/10.1016/j.ympev.2024.108109.

References

Allio, R., Schomaker-Bastos, A., Romiguier, J., Prosdocimi, F., Nabholz, B., Delsuc, F., 2020. MitoFinder: Efficient automated large-scale extraction of mitogenomic data in target enrichment phylogenomics. Mol. Ecol. Resour. 20, 892–905. https://doi.org/10.1111/1755-0998.13160.

Arnedo, M.A., Gillespie, R.G., 2006. Species diversification patterns in the Polynesian jumping spider genus *Havaika* Prószyński, 2001 (Araneae, Salticidae). Mol. Phylogenet. Evol. 41, 472–495. https://doi.org/10.1016/j.ympev.2006.05.012.

Azevedo, G.H.F., Parreiras, J.S., Bougie, T., Michalik, P., Wunderlich, J., Ramírez, M.J., 2021. Fossils constrain biogeographical history in a clade of flattened spiders with transcontinental distribution. J. Biogeogr. 1–17 https://doi.org/10.1111/jbi.14259.

Azevedo, G.H.F., Bougie, T., Carboni, M., Hedin, M., Ramírez, M.J., 2022. Combining genomic, phenotypic and Sanger sequencing data to elucidate the phylogeny of the two-clawed spiders (Dionycha). Mol. Phylogenet. Evol. 1–14 https://doi.org/10.1016/j.ympev.2021.107327.

Azevedo, G.H.F., Blair, J., Hedin, M., 2023. Evaluating possible anthropogenic impacts on gene flow and loss of genetic diversity in endangered Madla Cave Meshweaver spiders (Hahniidae, *Cicurina madla*). Conserv. Genet. 1–16 https://doi.org/10.1007/s10592-023-01561-y.

Bankevich, A., Nurk, S., Antipov, D., Gurevich, A.A., Dvorkin, M., Kulikov, A.S., Lesin, V. M., Nikolenko, S.I., Pham, S., Prjibelski, A.D., Pyshkin, A.V., Sirotkin, A.V., Vyahhi, N., Tesler, G., Alekseyev, M.A., Pevzner, P.A., 2012. SPAdes: A new genome assembly algorithm and its applications to single-cell sequencing. J. Comput. Biol. 19, 455–477. https://doi.org/10.1089/cmb.2012.0021.

Bidegaray-Batista, L., Arnedo, M.A., 2011. Gone with the plate: the opening of the Western Mediterranean basin drove the diversification of ground-dweller spiders. BMC Evol. Biol. 11, 317. https://doi.org/10.1186/1471-2148-11-317.

Bodner, M.R., Maddison, W.P., 2012. The biogeography and age of salticid spider radiations (Araneae: Salticidae). Mol. Phylogenet. Evol. 65, 213–240. https://doi.org/10.1016/j.ympev.2012.06.005.

Bolger, A.M., Lohse, M., Usadel, B., 2014. Trimmomatic: A flexible trimmer for Illumina sequence data. Bioinformatics 30, 2114–2120. https://doi.org/10.1093/bioinformatics/btu170.

Bougie, T.C., Brelsford, A., Hedin, M., 2021. Evolutionary impacts of introgressive hybridization in a rapidly evolving group of jumping spiders (F. Salticidae, *Habronattus americanus* group). Mol. Phylogenet. Evol. 161, 107165 https://doi.org/10.1016/j.ympev.2021.107165.

Bougie, T.C., Brelsford, A., Hedin, M., 2024. High sexual display trait diversity without measured genetic divergence in a montane hybrid zone involving young species (Araneae, Salticidae, *Habronattus americanus* subgroup). Insect Systemat. Divers. 8 https://doi.org/10.1093/isd/ixae001.

Castresana, J., 2000. Selection of conserved blocks from multiple alignments for their use in phylogenetic analysis. Mol. Biol. Evol. 17, 540–552. https://doi.org/10.1093/oxfordjournals.molbev.a026334.

Clouard, V., Bonneville, A., 2005. Ages of seamounts, islands, and plateaus on the Pacific plate. Special Pap. Geol. Soc. Am. 388, 71–90. https://doi.org/10.1130/0-8137-2388-4.71.

Dos Reis, M., Donoghue, P.C.J., Yang, Z., 2016. Bayesian molecular clock dating of species divergences in the genomics era. Nat. Rev. Genet. 17, 71–80. https://doi.org/10.1038/nrg.2015.8.

Douglas, J., Jimenez-Silva, C.L., Bouckaert, R., 2022. StarBeast3: Adaptive parallelized bayesian inference under the multispecies coalescent. Syst. Biol. 71, 901–916. https://doi.org/10.1093/sysbio/syac010.

Drummond, A., Rambaut, A., 2007. BEAST: Bayesian evolutionary analysis by sampling trees. BMC Evol. Biol. 7, 214. https://doi.org/10.1186/1471-2148-7-214.

Elias, D.O., Mason, A.C., Maddison, W.P., Hoy, R.R., 2003. Seismic signals in a courting male jumping spider (Araneae: Salticidae). J. Exp. Biol. 206, 4029–4039. https://doi.org/10.1242/jeb.00634.

Elias, D.O., Maddison, W.P., Peckmezian, C., Girard, M.B., Mason, A.C., 2012. Orchestrating the score: complex multimodal courtship in the *H. coecatus* group of *Habronattus* jumping spiders (Araneae: Salticidae). Biol. J. Linn. Soc. Lond. 105, 522–547. https://doi.org/10.1111/j.1095-8312.2011.01817.x.

Faircloth, B.C., 2016. PHYLUCE is a software package for the analysis of conserved genomic loci. Bioinformatics 32, 786–788. https://doi.org/10.1093/bioinformatics/btv646.

Garb, J.E., Gillespie, R.G., 2006. Island hopping across the central Pacific: Mitochondrial DNA detects sequential colonization of the Austral Islands by crab spiders (Araneae: Thomisidae). J. Biogeogr. 33, 201–220. https://doi.org/10.1111/j.1365-2699.2005.01398.x.

Gillespie, R.G., 2002. Biogeography of spiders on remote oceanic islands of the Pacific: Archipelagoes as stepping stones? J. Biogeogr. 29, 655–662. https://doi.org/10.1046/j.1365-2699.2002.00714.x.

Gillespie, R.G., Claridge, E.M., Goodacre, S.L., 2008. Biogeography of the fauna of French Polynesia: diversification within and between a series of hot spot archipelagos. Philosphical Transactions of the Royal Society B., 3335–3346. doi:10.1098/rstb.2008.012.

Gregory, T.R., Shorthouse, D.P., 2003. Genome sizes of spiders. J. Hered. 94, 285–290. https://doi.org/10.1093/jhered/esg070.

Griswold, C.E., 1987. A revision of the jumping spider genus *Habronattus* F. O. P.-Cambridge (Araneae; Salticidae), with phenetic and cladistic analyses. The University of California Publications in Entomology 107, 1–344.

Guindon, S., Dufayard, J.F., Lefort, V., Anisimova, M., Hordijk, W., Gascuel, O., 2010. New algorithms and methods to estimate maximum-likelihood phylogenies: Assessing the performance of PhyML 3.0. Syst. Biol. 59, 307–321. https://doi.org/10.1093/sysbio/syq010.

Heads, M., 2011. Old taxa on young Islands: A critique of the use of Island age to date Island-endemic clades and calibrate phylogenies. Syst. Biol. 60, 204–218. https://doi.org/10.1093/sysbio/syq075.

Hebets, E.A., Maddison, W.P., 2005. Xenophilic mating preferences among populations of the jumping spider *Habronattus pugillis* Griswold. Behav. Ecol. 16, 981–988.

Hedin, M., Derkarabetian, S., Alfaro, A., Ramírez, M.J., Bond, J.E., 2019. Phylogenomic analysis and revised classification of atypoid mygalomorph spiders (Araneae, Mygalomorphae), with notes on arachnid ultraconserved element loci. PeerJ 7, e6864.

Hedin, M., Foldi, S., Rajah-Boyer, B., 2020. Evolutionary divergences mirror Pleistocene paleodrainages in a rapidly-evolving complex of oasis-dwelling jumping spiders (Salticidae, Habronattus tarsalis). Mol. Phylogenet. Evol. 144, 106696 https://doi.org/10.1016/j.ympev.2019.106696.

Hembry, D.H., 2018. Evolutionary biogeography of the terrestrial biota of the Marquesas Islands, one of the world's remotest archipelagos. J. Biogeogr. 45, 1713–1726. https://doi.org/10.1111/jbi.13378.

Hill, D.E., Edwards, G.B., 2013. Origins of the North American jumping spiders (Araneae: Salticidae). Peckhamia 107, 1–67.

Ho, S.Y.W., Tong, K.J., Foster, C.S.P., Ritchie, A.M., Lo, N., Crisp, M.D., 2015. Biogeographic calibrations for the molecular clock. Biol. Lett. 11 https://doi.org/10.1098/rsbl.2015.0194.

Hohna, S., Landis, M.J., Heath, T.A., Boussau, B., Lartillot, N., Moore, B.R., Huelsenbeck, J.P., Ronquist, F., 2016. RevBayes: Bayesian phylogenetic inference using graphical models and an interactive model-specification language. Syst. Biol. 65, 726–736. https://doi.org/10.1093/sysbio/syw021.

Kalyaanamoorthy, S., Minh, B.Q., Wong, T.K.F., Von Haeseler, A., Jermiin, L.S., 2017. ModelFinder: Fast model selection for accurate phylogenetic estimates. Nat. Methods 14, 587–589. https://doi.org/10.1038/nmeth.4285.

Katoh, K., Standley, D.M., 2013. MAFFT multiple sequence alignment software version 7: Improvements in performance and usability. Mol. Biol. Evol. 30, 772–780. https://doi.org/10.1093/molbev/mst010.

Knope, M.L., Funk, V.A., Johnson, M.A., Wagner, W.L., Datlof, E.M., Johnson, G., Crawford, D.J., Bonifacino, J.M., Morden, C.W., Lorence, D.H., Wood, K.R., Meyer, J. Y., Carlquist, S., 2020. Dispersal and adaptive radiation of *Bidens* (Compositae) across the remote archipelagoes of Polynesia. J. Syst. Evol. 58, 805–822. https://doi.org/10.1111/jse.12704.

Kulkarni, S., Wood, H., Lloyd, M., Hormiga, G., 2020. Spider-specific probe set for ultraconserved elements offers new perspectives on the evolutionary history of spiders (Arachnida, Araneae). Mol. Ecol. Resour. 20, 185–203. https://doi.org/10.1111/1755-0998.13099.

Landis, M.J., 2017. Biogeographic dating of speciation times using paleogeographically informed processes. Syst. Biol. 66, 128–144. https://doi.org/10.1093/sysbio/syw040.

Landis, M.J., Matzke, N.J., Moore, B.R., Huelsenbeck, J.P., 2013. Bayesian analysis of biogeography when the number of areas is large. Syst. Biol. 62, 789–804. https://doi.org/10.1093/sysbio/syt040.

Landis, M.J., Freyman, W.A., Baldwin, B.G., 2018. Retracing the Hawaiian silversword radiation despite phylogenetic, biogeographic, and paleogeographic uncertainty. Evolution 72, 2343–2359. https://doi.org/10.1111/evo.13594.

Landis, M.J. 2021. Biogeographic dating of phylogenetic divergence times using priors and processes. In: Ho, S.Y.W. (Eds), The Molecular Evolutionary Clock: Theory and Practice. Springer, Cham, pp. 135–155. doi:10.1007/978-3-030-60181-2_9.

Leduc-Robert, G., Maddison, W.P., 2018. Phylogeny with introgression in *Habronattus* jumping spiders (Araneae: Salticidae). BMC Evol. Biol. 18, 24. https://doi.org/10.1186/s12862-018-1137-x.

Li, H., Handsaker, B., Wysoker, A., Fennell, T., Ruan, J., Homer, N., Marth, G., Abecasis, G., Durbin, R., 2009. The sequence alignment/map format and SAMtools. Bioinformatics 25, 2078–2079. https://doi.org/10.1093/bioinformatics/btp352.

Li, H., 2013. Aligning sequence reads, clone sequences and assembly contigs with BWA-MEM. Available at: http://arxiv.org/abs/1303.3997.

Logunov, D.V., Marusik, Y.M., Rakov, S.Y., 1999. A review of the genus *Pellenes* in the fauna of Central Asia and the Caucasus (Araneae, Salticidae). J. Nat. Hist. 33, 89–148.

Lowrie, D.C., Gertsch, W.J., 1955. A list of the spiders of the Grand Teton Park area, with descriptions of some new North American spiders. Am. Mus. Novit. 1736, 1–29.

Maddison, W.P., 2015. A phylogenetic classification of jumping spiders (Araneae: Salticidae). J. Arachnol. 43, 231–292. https://doi.org/10.1636/arac-43-03-231-292.

Maddison, W.P., 2017. New species of *Habronattus* and *Pellenes* jumping spiders (Araneae: Salticidae: Harmochirina). ZooKeys 646, 45–72. https://doi.org/10.3897/zookeys.646.10787.

Maddison, W.P., Maddison, D.R., 2015. Mesquite: a modular system for evolutionary analysis. Version 3.04. *Available at: mesquiteproject.org/mesquite/download/download.html.*

Maddison, W.P., McMahon, M.M., 2000. Divergence and reticulation among montane populations of the jumping spider *Habronattus pugillis* Griswold. Syst. Biol. 49, 400–421. https://doi.org/10.1080/10635159950127312.

Maddison, W.P., Bodner, M.R., Needham, K., 2008. Salticid spider phylogeny revisited, with the discovery of a large Australasian clade (Araneae: Salticidae). Zootaxa 1893, 49–64. https://doi.org/10.11646/zootaxa.1893.1.3.

Maddison, W.P., Leduc-Robert, G., 2013. Multiple origins of sex chromosome fusions correlated with chiasma localization in *Habronattus* jumping spiders (Araneae: Salticidae). Evolution 67, 2258–2272. https://doi.org/10.1111/evo.12109.

Maddison, W.P., Beattie, I., Marathe, K., Ng, P.Y.C., Kanesharatnam, N., Benjamin, S.P., Kunte, K., 2020. A phylogenetic and taxonomic review of Baviine jumping spiders (Araneae, salticidae, Baviini). ZooKeys 2020, 27–97. https://doi.org/10.3897/zookeys.1004.57526.

Maddison, W.P., Hedin, M.C., 2003a. Phylogeny of *Habronattus* jumping spiders (Araneae: Salticidae), with consideration of genitalic and courtship evolution. Syst. Entomol. 28, 1–21. https://doi.org/10.1046/j.1365-3113.2003.00195.x.
Maddison, W.P., Hedin, M.C., 2003b. Jumping spider phylogeny (Araneae: Salticidae). Invertebr. Syst. 17, 529–549. https://doi.org/10.1071/IS02044.
Maddison, W.P., 2024. *Hivanua*, a new genus of harmochirine jumping spiders from the Marquesas Islands (Araneae: Salticidae: Harmochirina). ZooKeys, in press.
Magalhães, I.L.F., Azevedo, G.H.F., Michalik, P., Ramírez, M.J., 2020. The fossil record of spiders revisited: implications for calibrating trees and evidence for a major faunal turnover since the Mesozoic. Biol. Rev. 95, 184–217. https://doi.org/10.1111/brv.12559.
Mai, U., Mirarab, S., 2018. TreeShrink: Fast and accurate detection of outlier long branches in collections of phylogenetic trees. BMC Genomics 19. https://doi.org/10.1186/s12864-018-4620-2.
Marathe, K., Tripathi, R., Sudhikumar, A.V., Maddison, W.P., 2024. Phylogenomic placement and revision of *Iranattus* jumping spiders (Salticidae, Plexippini, Plexippina). Zoosystematics and Evolution 100, 531–542. https://doi.org/10.3897/zse.100.122034.
Massana, K.A., Beaulieu, J..M, Matzke, N.J., O'Meara, B.C., 2015. Non-null Effects of the Null Range in Biogeographic Models: Exploring Parameter Estimation in the DEC Model. bioRxiv, 026914. doi:10.1101/026914.
Masta, S.E., Maddison, W.P., 2002. Sexual selection driving diversification in jumping spiders. Proc. Natl. Acad. Sci. 99, 4442–4447.
Matzke, N.J., 2013. Probabilistic historical biogeography: New models for founder-event speciation, imperfect detection, and fossils allow improved accuracy and model-testing. Front. Biogeogr. 5 https://doi.org/10.21425/F5FBG19694.
Matzke, N.J., 2022. Statistical comparison of DEC and DEC+J is identical to comparison of two ClaSSE submodels, and is therefore valid. J. Biogeogr. 49, 1805–1824. https://doi.org/10.1111/jbi.14346.
Minh, B.Q., Nguyen, M.A.T., von Haeseler, A., 2013. Ultrafast approximation for phylogenetic bootstrap. Mol. Biol. Evol. 30, 1188–1195. https://doi.org/10.1093/molbev/mst024.
Monjaraz-Ruedas, R., Mendez, R.W., Hedin, M., 2023. Species delimitation, biogeography, and natural history of dwarf funnel web spiders (Mygalomorphae, Hexurellidae, *Hexurella*) from the United States / Mexico borderlands. ZooKeys 2023, 109–157. https://doi.org/10.3897/zookeys.1167.103463.
Mooers, A., Schluter, D., 1999. Reconstructing ancestor states with maximum likelihood: Support for one- and two-rate models. Syst. Biol. 48, 623–633. https://doi.org/10.1080/106351599260193.
Nel, A., de Ploëg, G., Millet, J., Menier, J.J., Waller, A., 2004. The French ambers: A general conspectus and the Lowermost Eocene amber deposit of Le Quesnoy in the Paris Basin. Geol. Acta 2, 3–8.
Newton, L.G., Starrett, J., Jochim, E.E., Bond, J.E., 2023. Phylogeography and cohesion species delimitation of California endemic trapdoor spiders within the *Aptostichus icenoglei* sibling species complex (Araneae: Mygalomorphae: Euctenizidae). Ecol. Evol. 13, e10025.
Nguyen, L.T., Schmidt, H.A., Von Haeseler, A., Minh, B.Q., 2015. IQ-TREE: a fast and effective stochastic algorithm for estimating maximum-likelihood phylogenies. Mol. Biol. Evol. 32, 268–274. https://doi.org/10.1093/molbev/msu300.
Ogilvie, A., Bouckaert, R.R., Drummond, A.J., 2017. StarBEAST2 brings faster species tree inference and accurate estimates of substitution rates. Mol. Biol. Evol. 34, 2101–2114. https://doi.org/10.1093/molbev/msx126.
Peckham, G.W., Peckham, E.G., 1889. Observations on sexual selection in spiders of the family Attidae. Occasional Papers of the Wisconsin Natural History Society 1, 1–60.
Peckham, G.W., Peckham, E.G., 1890. Additional observations on sexual selection in spiders of the family Attidae, with some remarks on Mr Wallace's theory of sexual ornamentation. Occasional Papers of the Wisconsin Natural History Society 1,117–151.
Peckham, G.W., Peckham, E.G. 1909. Revision of the Attidae of North America. Transactions of the Wisconsin Academy of Sciences, Arts and Letters 16, 355–655.
Piacentini, L.N., Ramírez, M.J., 2019. Hunting the wolf: A molecular phylogeny of the wolf spiders (Araneae, Lycosidae). Mol. Phylogenet. Evol. 136, 227–240. https://doi.org/10.1016/j.ympev.2019.04.004.
Prószyński, J., 2002. Remarks on Salticidae (Aranei) from Hawaii, with description of *Havaika* - gen. nov. Arthropoda Selecta 10, 225–241.
Prószyński, J., 2008. A Survey of *Havaika* (Aranei: Salticidae), and endemic genus from Hawaii, including descriptions of new species. Arthropoda Selecta 16, 195–213.
Prószyński, J., 2016. Delimitation and description of 19 new genera, a subgenus and a species of Salticidae (Araneae) of the world. Ecol. Montenegrina 7, 4–32.
Rambaut, A., Drummond, A.J., Xie, D., Baele, G., Suchard, M.A., 2018. Posterior summarization in Bayesian phylogenetics using Tracer 1.7. Syst. Biol. 67, 901–904. https://doi.org/10.1093/sysbio/syy032.
Rannala, B., 2002. Identifiability of parameters in MCMC Bayesian inference of phylogeny. Syst. Biol. 51, 754–760. https://doi.org/10.1080/10635150290102429.
Ree, R.H., Sanmartín, I., 2018. Conceptual and statistical problems with the DEC+J model of founder-event speciation and its comparison with DEC via model selection. J. Biogeogr. 45, 741–749. https://doi.org/10.1111/jbi.13173.
Ree, R.H., Smith, S.A., 2008. Maximum likelihood inference of geographic range evolution by dispersal, local extinction, and cladogenesis. Syst. Biol. 57, 4–14. https://doi.org/10.1080/10635150701883881.
Rivera, C., Hedin, M., Mason, A.C., Maddison, W.P., Elias, D.O., 2021. Complex courtship in the *Habronattus clypeatus* group (Araneae: Salticidae). J. Arachnol. 48, 221–232.
Rybczynski, N., Gosse, J.C., Richard Harington, C., Wogelius, R.A., Hidy, A.J., Buckley, M., 2013. Mid-Pliocene warm-period deposits in the High Arctic yield insight into camel evolution. Nat. Commun. 4, 1–9. https://doi.org/10.1038/ncomms2516.
Schenk, J.J., 2016. Consequences of secondary calibrations on divergence time estimates. PLoS One 11. https://doi.org/10.1371/journal.pone.0148228.
Stamatakis, A., 2014. RAxML Version 8: A tool for phylogenetic analysis and post-analysis of large phylogenies. Bioinformatics 30, 1312–1313. https://doi.org/10.1093/bioinformat- ics/btu033.
Starrett, J., Derkarabetian, S., Hedin, M., Bryson, R.W., McCormack, J.E., Faircloth, B.C., 2017. High phylogenetic utility of an ultraconserved element probe set designed for Arachnida. Mol. Ecol. Resour. 17, 812–823. https://doi.org/10.1111/1755-0998.12621.
Sukumaran, J., Holder, M.T., 2010. DendroPy: A Python library for phylogenetic computing. Bioinformatics 26, 1569–1571. https://doi.org/10.1093/bioinformatics/btq228.
Tao, Q., Tamura, K., Kumar, S. 2020. Efficient Methods for Dating Evolutionary Divergences. In: Ho, S.Y.W. (eds), The Molecular Evolutionary Clock. Springer: Cham. pp. 197–219. doi:10.1007/978-3-030-60181-2_12.
Taylor, L.A., McGraw, K.J., 2013. Male ornamental coloration improves courtship success in a jumping spider, but only in the sun. Behav. Ecol. 24, 955–967.
Taylor, L.A., Amin, Z., Maier, E.B., Byrne, K.J., Morehouse, N.I., 2016. Flexible color learning in an invertebrate predator: *Habronattus* jumping spiders can learn to prefer or avoid red during foraging. Behav. Ecol. 27, 520–529. https://doi.org/10.1093/beheco/arv182.
Tumescheit, C., Firth, A.E., Brown, K., 2022. CIAlign: A highly customisable command line tool to clean, interpret and visualise multiple sequence alignments. PeerJ. https://doi.org/10.7717/peerj.12983.
Van Dam, M.H., Henderson, J.B., Esposito, L., Trautwein, M., 2021. Genomic characterization and curation of UCEs improves species tree reconstruction. Syst. Biol. 70, 307–321. https://doi.org/10.1093/sysbio/syaa063.
Xie, W., Lewis, P.O., Fan, Y., Kuo, L., Chen, M.H., 2011. Improving marginal likelihood estimation for bayesian phylogenetic model selection. Syst. Biol. 60, 150–160. https://doi.org/10.1093/sysbio/syq085.
Zhang, J., Li, Z., Lai, J., Zhang, Z., Zhang, F., 2023. A novel probe set for the phylogenomics and evolution of RTA spiders. Cladistics 1–13. https://doi.org/10.1111/cla.12523.
Zhang, J., Maddison, W.P., 2013. Molecular Phylo genetics and Evolution Molecular phylogeny, divergence times and biogeography of spiders of the subfamily Euophryinae (Araneae: Salticidae). Mol. Phylogenet. Evol. 68, 81–92. https://doi.org/10.1016/j.ympev.2013.03.017.
Zhang, C., Rabiee, M., Sayyari, E., Mirarab, S., 2018. ASTRAL-III: Polynomial time species tree reconstruction from partially resolved gene trees. BMC Bioinf. 19, 15–30. https://doi.org/10.1186/s12859-018-2129-y.
Zurek, D.B., Cronin, T.W., Taylor, L.A., Byrne, K., Sullivan, M.L.G., Morehouse, N.I., 2015. Spectral filtering enables trichromatic vision in colorful jumping spiders. Curr. Biol. 25, R403–R404.